

STUDY OF SURFACE AND MECHANICAL PROPERTIES OF CHROMIUM
THIN FILM BY RF DIODE SPUTTERING

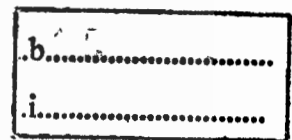


E076489

Mr. Theerachai Sae-Jong



เลขหมู่.....
เลขทะเบียน..... 76489
วัน,เดือน,ปี..... 25 ส.ค. 2557



THESIS SUBMITTED IN PARTIAL FULFILLMENT OF THE REQUIREMENT
FOR THE MASTER DEGREE OF ENGINEERING IN DATA STORAGE TECHNOLOGY
COLLEGE OF DATA STORAGE TECHNOLOGY AND APPLICATION
KING MONGKUT'S INSTITUTE OF TECHNOLOGY LADKRABANG

2013

KMITL-2012-IC-M-005-008



COPYRIGHT 2013

SCHOOL OF GRADUATE STUDIES

KING MONGKUT'S INSTITUTE OF TECHNOLOGY LADKRABANG

This material is reserved for educational use only, not allowed for commercial use.

หัวข้อวิทยานิพนธ์	การศึกษาพื้นผิวและสมบัติเชิงกลของโครเมียมฟิล์มด้วยระบบอาร์เอฟสปัตเตอริง
ชื่อนักศึกษา	นายธีรชัย แซ่จง
รหัสประจำตัว	53600603
ปริญญา	วิศวกรรมศาสตรมหาบัณฑิต
สาขาวิชา	เทคโนโลยีบัณฑิตข้อมูล
อาจารย์ผู้ควบคุมวิทยานิพนธ์	รศ.ดร.วิสุทธิ์ ฐิติรุ่งเรือง

บทคัดย่อ

อนุภาคปนเปื้อน ซึ่งก่อตัวขึ้นในช่วงการเคลือบฟิล์มด้วยพลาสมาก่อให้เกิดปัญหาสำหรับกระบวนการผลิตฟิล์มบาง การก่อตัวและการเคลื่อนที่ของอนุภาคในพลาสมากระบวนการเคลือบและพลาสมากระบวนการกัด ได้แสดงถึงความคล้ายคลึงกันของส่วนของการปลูกฟิล์มและถูกปนเปื้อน กลไกนี้อาจเป็นส่วนที่พบได้ปกติในกระบวนการสปัตเตอริงหลายรูปแบบ เครื่องมือวัดอนุภาคด้วยเลเซอร์ถูกใช้เพื่อพิจารณาและวัดขนาดของอนุภาคบนพื้นผิวเวเฟอร์หลังจากเคลือบฟิล์มภายนอกแชนเบอร์ FE-SEM และ เทคนิค EDX ถูกใช้สำหรับอธิบายลักษณะของอนุภาค การทดลองได้ทำการจำแนกประเภทออกเป็นสามส่วนกลุ่มทดลอง กลุ่มแรกตั้งค่าความดันการเคลือบฟิล์มที่ 4, 8, 20 และ 30 มิลลิทอร์ โดยที่ตัวแปรอื่นถูกควบคุม กลุ่มที่สองตั้งค่าลบไบอัสความต่างศักย์ของสับเสตรความดันที่ 160, 120, 80 และ 40 โวลท์ กลุ่มที่สาม ตั้งค่าระยะห่างของอิเล็กโทรดที่ 1, 1.3 และ 1.6 จากผลการทดลอง เงื่อนไขที่เหมาะสมสำหรับการได้ค่าน้อยที่สุดของอนุภาคคอนแทมมิเนชันคือที่ 8 มิลลิทอร์ ไบอัสโวลท์เทจลบ 40 โวลท์ และระยะห่างระหว่างสับเสตรกับทาร์เก็ต 1.6 นิ้ว ตามที่ผลของ EDX ค่าคอนแทมมิเนชันบนผิวฟิล์มอาจเกิดจากแหล่งที่มาหลายลักษณะเช่น ทาร์เก็ต สับเสตร และส่วนประกอบของระบบสปัตเตอริง จากนั้นนำฟิล์มบางโครเมียมที่เคลือบด้วยค่าต่างๆกันไปวัดค่าความขรุขระ ความหนาฟิล์มของความไม่เป็นแบบเดียวกันพื้นผิวลักษณะทางสัณฐาน ความแข็งของฟิล์ม และนาโนอินเดนเทคเทคนิคถูกศึกษาในค่าตัวแปรต่างประเภท ซึ่งพบว่าเมื่อให้ค่าความต่างศักย์ลบ 160 โวลท์ ความดัน 8 มิลลิทอร์ ระยะห่างระหว่างอิเล็กโทรด 1.6 นิ้ว ค่าความขรุขระที่วัดด้วยค่าเฉลี่ยความขรุขระ R_a 3.7 นาโนเมตร และมีค่าความแข็งที่ 9.5 กิกกะปาสคาล (GPa) ซึ่งเกิดจากการจัดเรียงตัวเป็นโครงสร้างผลึกเกรนเพิ่มขึ้น

คำสำคัญ: โครเมียม/ อาร์เอฟไดโอด สปัตเตอริง/พีเอ็ม (Fe-SEM) /อะตอมมิกฟอร์ซไมโครสโคป (AFM)

INDEPENDENT STUDY TITLE STUDY OF SURFACE AND MECHANICAL PROPERTIES
OF CHROMIUM THIN FILM BY RF DIODE SPUTTERING

STUDENT Name Theerachai Sae-jong

STUDENT ID. 53600603

Degree Master of Engineer

Program College Data Storage Technology and Applications

ADVISOR Assoc. Prof. Dr. Wisut Titiroongruang

Abstract

Particulate contamination generated during plasma deposition caused violent problems for the production of thin films. Particle formation and transportation in plasma deposition process and plasma etching process show similarities in term of growth and trapping. This mechanism may be universal to many sputtering processes. KLA machine was used to scan and measure size of particle on wafer surface after coating outside sputtering chamber. FE-SEM and EDX technique were used for characterizing particles. The experiments can be categorized into 3 groups. First group varies processing pressure at 4, 8, 20, and 30 mTorr while other parameters were controlled. Second group varies substrate negative biased voltage at 40, 80, 120, and 160 V. Third varies gap distance between two electrodes at 1, 1.3 and 1.6 inch. From the experimental results, the optimum conditions for obtaining the lowest level of particulate contamination is 8 mTorr, 40 V and 1.6 inch for process pressure, substrate bias voltage and gap distance between the substrate and target. According to EDX results, the contamination on film surface may come from various sources, such as from target, substrate, and sputtering system component. After that surface roughness, surface thickness non-uniformity, surface morphology, surface hardness and Nano-indentation were observed in various process parameters, the optimum conditions result from parameter negative bias voltage 160V 8 mTorr deposit pressure and 1.6 inch distance between two electrodes given the good roughness with R_a 3.7 nm 9.5 GPa hardness and excellent surface hardness which have given increasing grain structure.

Keywords: Chromium/RF diode sputtering/FE-SEM/AFM

ACKNOWLEDGEMENT

To be completeness of this thesis. I would like to thank all of these following persons for their supports and helpfulness in my thesis.

First, I would like to thank Assoc. Prof. Dr. Wisut Titiroongruang, my advisor who always provided a lot of sustained guidance, many indispensable advices and reviews. They spend a lot of their time for teaching and discussion. Completion of my thesis may not be achieved without their supports and advices.

Second, I would like to thank western digital company, Mr. Pricha Leelanukrom who give company scholarship to me and also Mrs. Panita Ngamprasert who supports many things during studying time, I got a lot of good experience and excellent knowledge from data storage technology.

Third, Thank to Mr. Narong khamdee and Miss. Sonthirat krunkrong; my bosses and all colleagues. During working time, it is a touch time that someone is working and studying in the same time. Completion of my thesis also may not be achieved without understanding.

Fourth, thank to all DSTAR professors who give me many skills and knowledge. They always welcome for advice and teaching in over time.

Finally, I would like to thank to my family that everyone gives unfailing encouragement; especially, my parents. I would like to dedicate this thesis to them and say thank to everyone again for encouraging me to pursue higher education.

Theerachai Sae-jong

TABLE OF CONTENTS

	Page
THAI ABSTRACT.....	I
ENGLISH ABSTRACT.....	II
ACKNOWLEDGEMENT.....	III
TABLE OF CONTENTS.....	IV
LIST OF TABLES.....	V
LIST OF FIGURES.....	VII
CHAPTER 1 INTRODUCTION.....	1
1.1 Statement and significance of problems.....	1
1.2 Objectives	2
1.3 Scope and limitations.....	3
1.4 Benefit.....	3
CHAPTER 2 Theory.....	4
2.1 Contamination.....	4
2.2 Physical vapor deposition (PVD) sputtering	4
2.2.1 Ion-surface reactions.....	5
2.2.2 Basic plasma physics.....	6
2.2.3 RF Diode sputtering.....	7
2.2.4 Sputtering mechanics.....	10
2.2.5 Description of plasma.....	11
2.2.6 RF diode sputtering equipment	12
2.2.6.1 Pressure.....	13
2.2.6.2 Deposition distribution.....	13
2.2.6.3 Power.....	13
2.2.6.4 Cathode.....	13
2.2.6.5 Contamination.....	14
2.2.6.6 Deposition control.....	14
2.2.6.7 Sputter source.....	15
2.2.6.8 Mechanical properties of Chromium films	16
2.2.6.9 Hardness and Elastic modulus	17
2.3 Characterization of Cr film.....	18
2.3.1 Scanning electron microscope (SEM).....	18
2.3.2 Atomic force microscopy (AFM).....	18
2.4 Thickness non-uniformity measurement	20

This material is for personal use only, not allowed for commercial use.

Forbidden to modify the content, and cite the document when use.

TABLE OF CONTENTS (Continued)

	Page
2.5 Laser techniques	20
2.6 Literature reviews.....	22
CHAPTER 3 EXPERIMENTAL DETAILS.....	24
3.1 Materials.....	24
3.1.1 Chromium target.....	24
3.1.2 AlTiC substrate.....	24
3.1.3 Gas.....	24
3.1.4 The background deposit pressure.....	24
3.2 Instruments.....	24
3.3 Flow chart of the experiments.....	25
3.4 Sample preparation	26
3.4.1 AlTiC substrate.....	26
3.4.2 Typical vacuum deposition system	28
3.4.3 Step of chromium film hard coating by RF diode sputtering.....	28
3.4.4 Sputter-etch step	30
3.4.5 Pre-sputter step	31
3.4.6 Deposition step	32
3.4.7 Vacuum gauge controller	33
3.4.8 Thermocouple gauge	33
3.4.9 MKS Baratron gauge.....	33
3.5 Characterization of Chromium film.....	34
3.5.1 Film non uniformity measurement by using micro	34
3.5.2 Surface hardness	34
3.5.3 Thickness non-uniformity measurement	34
3.6 Experiment varied substrate bias voltage.....	35
3.7 Conclusion.....	36
CHAPTER 4 RESULTS AND results.....	37
4.1 The effect of plasma parameter on surface morphology of wafers.....	37
4.1.1 Various substrate bias voltage.....	37
4.1.2 Various deposit pressure.....	38
4.1.3 Various distance between two electrode	38
4.2 Study of the film thickness non-uniformity.....	41

This material is reserved for educational use only, not allowed for commercial use.

Forbidden to modify the content, and cite the document when use.

TABLE OF CONTENTS (Continued)

	Page
4.2.1 Various substrate bias voltages.....	41
4.2.2 Surface diagram with V_b -40V	41
4.2.3 Surface diagram with V_b -80V	42
4.2.4 Surface diagram with V_b -120V	43
4.2.5 Surface diagram with V_b -160V	43
4.2.6 Surface diagram with pressure at 4 mT.....	45
4.2.7 Surface diagram with pressure at 8 mT.....	45
4.2.8 Surface diagram with pressure at 20 mT.....	46
4.2.9 Surface diagram with pressure at 30 mT.....	46
4.2.10 Surface diagram with distance 1inch.....	47
4.2.11 Surface diagram with distance 1.3inch.....	48
4.2.12 Surface diagram with distance 1.6inch.....	49
4.3 Surface hardness.....	50
4.3.1 Hardness results by various negative bias voltage	50
4.3.2 Hardness results by various deposit pressure.....	51
4.4 Surface roughness and morphology of Cr film	52
4.5 SEM micrograph surface grain the fractured surface of Cr film.....	55
CHAPTER 5 CONCLUSIONS AND SUGGESTION.....	59
5.1 Conclusion.....	59
5.2 Suggestion for further work.....	60
REFERENCES.....	61
APPENDIX A.....	63
AUTHOR BIOGRAPHY.....	68

List of tables

Table	Page
2.1 Material Temperature for given vapor pressure	17
4.1 Compare uniformity vs various bias voltage and standard deviation of each parameter.....	41
4.2 Compare uniformity various deposit pressure parameter	47
4.3 Compares uniformity various distances between two electrodes	49
4.4 Hardness comparison by various substrate bias voltages.....	50
4.5 Surface hardness of Cr film as function of deposit pressure.....	50
4.6 Arithmetic mean of the area roughness average roughness R root mean square and R_{max}	54



List of figures

Figure	Page
2.1 Ion-surface interactions.....	5
2.2 The behavior of the potential between two plates, on grounded anode and one cathode at negative potential, immersed in a plasma V_p is the plasma potential	6
2.3 Schematic illustration of RF Diode Sputtering deposition.....	8
2.4 Dependence of the sputtering yield of several elements (ordered according their position in the periodic table) calculated using SRIM (initial conditions: 300eV Ar, other input parameters where set at the standard values given by SRIM: lattice binding energy, surface binding energy displacement energy, and normal incidence.....	9
2.5 Corona discharge point attachment for electrophorus.....	11
2.6 A typical V/I plot of a glow discharge. The main characteristics of the discharge, the voltage current characteristic and the structure of the discharge depend on geometry of the electrode, the gas used, the pressure and the electrode material	12
2.7 RF diode sputter deposition system consists of a vacuum chamber, a sputter source, vacuum sensors, a substrate holder, and pumping system	14
2.8 Schematic of Comteh coating machine	14
2.9 Force versus displacement curve on film showing typical response of elastic-material and resulting in-situ SPM image of surface after quasi-static indentation showing residue indentation impression	18
2.10 AFM detect the sample by using cantilever	19
2.11 CRDS schematic laser particle count.....	21
3.1 Schematic of Alcatel Comptech 2460 RF sputtering.....	25
3.2 Schematic of target and substrate electrode	26
3.3 Substrate position diagram in sputtering chamber	27
3.4 The working area contains screen views depicting the system	29
3.5 Vacuum system diagram when the system pump down to base pressure	30
3.6 Vacuum pump system diagram of RF diode sputtering during pre-etch	31
3.7 Vacuum pump system diagram of RF diode sputtering on pre-sputter step	32
3.8 Vacuum pump system diagram of RF diode sputtering deposit step	33
3.9 Thickness uniformity over 6" wafer substrate for provide sample.....	34
4.1 Surface defect with various substrate bias voltage parameter	37
4.2 Surface defect with various deposit pressure parameter	38
4.3 Surface defect with various distances between two electrodes.....	39

This material is reserved for educational use only, not allowed for commercial use.

Forbidden to modify the content, and cite the document when use.

List of figures (Continued)

Figure	Page
4.4 Point defect is captured with high power microscopy and (b) SEM image show hole inside Cr film with approximately 5 μm diameter The EDX detail at point 1 show composition of Cr, but at point 2 show composition of C substrate.....	39
4.5 (a) Dark spot contamination is taken under high power microscopy. (b)SEM image show approximately 10 μm length. The EDX detail at point 1 show a composition of Cr film. But at point 2 show Cr and C	40
4.6 Particulate contamination results with EDX mode.....	40
4.7 Surface diagram of chromium film with bias voltage -40V.....	42
4.8 Surface diagram of chromium film with bias voltage -80V.....	42
4.9 Surface diagram of chromium film with bias voltage -120V.....	43
4.10 Surface diagram of chromium film with bias voltage -160V.....	43
4.11 Compare uniformity vs various bias voltage and standard deviation of bias parameter.	44
4.12 Surface diagram of chromium film with deposit pressure 4 mT.....	45
4.13 Surface diagram of chromium film with deposit pressure 8 mT.....	45
4.14 Surface diagram of chromium film with deposit pressure 20 mT.....	45
4.15 Surface diagram of chromium film with deposit pressure 30 mT.....	46
4.16 Compare uniformity vs various deposit pressure and standard deviation of parameter.....	47
4.17 Surface diagram of chromium film with distance between two electrodes 1 inch.....	48
4.18 Surface diagram of chromium film with distance between two electrodes 1.3 inch.....	48
4.19 Surface diagram of chromium film with distance between two electrodes 1.6 inch.....	49
4.20 Compare uniformity vs various distances between two electrodes and standard deviation of each parameter.....	50
4.21 Compare hardness results vs various bias voltage parameters.....	51
4.22 Compare loading force and normal displacement by various deposit pressure.....	51
4.23 Surface roughness of bias voltage -40 V.....	52
4.24 Surface roughness of bias voltage -80 V.....	53
4.25 Surface roughness of bias voltage -120 V.....	53
4.26 Surface roughness of bias voltage -160 V.....	53
4.27 The roughness of chromium film deposit on ALTIC substrate by various bias voltage.....	54

This document is for educational use only, not allowed for commercial use.

Forbidden to modify the content, and cite the document when use.

List of figures (Continued)

Figure	Page
4.28 Grain of chromium film with substrate bias -160V, SEM image 20,000 X and 50,000X magnification.	56
4.29 Grain of chromium film with substrate bias -120V, SEM image 20,000 X and 50,000X magnification	56
4.30 Grain of chromium film with substrate bias -80V, SEM image 20,000 X and 50,000X magnification	56
4.28 Grain of chromium film with substrate bias -40V, SEM image 20,000 X and 50,000X magnification	57



CHAPTER 1

Introduction

1.1 Statement and Significance of Problems

Particulate contamination generated during plasma deposition caused serious problems for the production of thin films. Particle formation and transportation in plasma deposition process and plasma etching process show similarities in term of growth and trapping. Nano mechanical properties are needed a develop method to understand surface and interfacial phenomena on nano scale, such as the micro/nanostructure used in wafer hard coating to do pattern on hardmask coating in slider fabrication magnetic storage system and other industrial application. Particle present in sputter deposition process are expected to have zero particles on deposition step. The difference in the rates of electron and ion collisions caused particulate contamination on film. Quantity of contamination depends on the electron density and temperature. The charge on particulates combined with the negative field at the sheath boundary can result in suspended particles which have transportation significant distance in plasma.

The development of engineering demands the requirement of materials with better surface mechanical properties, resistance to frictional wear, and resistance to corrosion roughness and good uniformity. Theses demand can be satisfied by applying various coating parameter of Physical vapor deposition (PVD) and surface engineering techniques. Chromium film was used hard coating PVD method which can result in eventual micro contamination on film. Consequently, these studied to reduce contamination on film with PVD coating and limit the applications where a hard surface load wafer for do mask patterning is required. These layers improve essentially the performance properties and widen significantly the application range of the chromium film hard coating which is now being increasingly used in electronic industry [1].

Chromium thin film is deposited by various parameter deposition of physical vapor deposition (PVD).This techniques have developed in practical applications. It is exhibits excellent wear resistance and good corrosion resistance. However Chromium hard coating has been proposed to be a hard coating, wear-resistance chemical inert for ceramic coating. In this study, Chromium film contamination was observed by using laer particle count machine (KLA). Surface roughness were studied with the atomic force microscope (AFM) was employed to conduct the nano hardness roughness. SEM used view grain size of hard coating Chromium film the nano

This material is reserved for educational use only, not allowed for commercial use.

Forbidden to modify the content, and cite the document when use.

hardness and film resistance. Basically RF Diode sputtering utilizes an AC current to cathode Chromium target. Inert gas (Argon) plasma is initiated and maintained between the target and the substrate by RF power source at considerably lower pressure 5-20 mTorr. The Ar^+ ion accelerated across the target shield bombard substrate and result in sputtering of metal atom from the target. These sputtered atoms then transported to the substrate and deposited. Plasma potentials are developed at both the target and substrate in RF discharge and the positive ion also impact the substrate because of substrate shield potential.

There is ever increasing interest in the applications of chromium in such sectors as automotive, electronic industry, in which tribological behavior is often a major concern. In general, in the preparation of chromium films higher substrate temperature process parameters like operating pressure[7], substrate biasing [2], nitrogen addition [3],etc., have found to influence the structural transformation in several ways, in addition to the contamination. However, it is necessary to look at the influence of all the process parameters and overall effect on the surface of chromium film to have a better understanding of the structure and mechanical property. In this studied, we studied the influence of process parameter on the contamination uniformity roughness hardness of RF diode sputter deposited chromium films. RF sputter deposition is known low pressure sputtering with independent control over the energy and flux.

1.2 Objectives

1.2.1 Study the method of chromium film coating by using RF diode sputtering.

1.2.2 To study surface defect of chromium film on ALTiC substrate by using RF diode sputtering.

1.2.3 To study optimum condition of deposition parameter.

1.2.4 Study mechanical properties of chromium film on ALTiC substrate wafer with various with RF diode sputtering technique.

1.3 Scope and limitations

From this study, we focused on the contamination on ALTiC substrate 6 inch diameter with various negative substrate voltage at 40, 80, 120, and 160 Volt, deposit pressure at 4, 8, 20, 30 mT and various distance between two electrode 1, 1.3 and 1.6 inch

1.3.1 Coat chromium film with RF diode sputtering on Alumium Titanium Carbide (ALTiC) substrate

This material is reserved for educational use only, not allowed for commercial use.

Forbidden to modify the content, and cite the document when use.

1.3.2 To study optimum of process parameter of chromium film coating with RF diode sputtering

- Substrate bias voltage
- Deposit pressure
- Distance between two electrode

1.3.3 To study chromium film surface contamination and mechanical properties such as hardness roughness uniformities grain size.

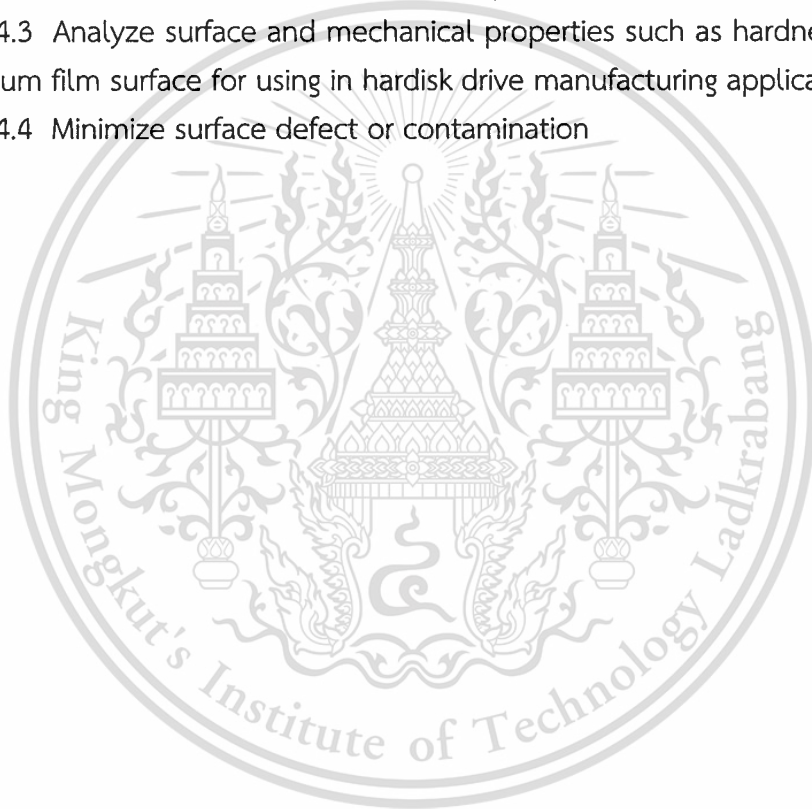
1.4 Benefit

1.4.1 To study chromium film coating method by using RF diode sputtering

1.4.2 To understand coating chromium properly

1.4.3 Analyze surface and mechanical properties such as hardness roughness of chromium film surface for using in hardisk drive manufacturing application

1.4.4 Minimize surface defect or contamination



Chapter 2

Theory

2.1 Contamination

Particles contaminate is generated in plasma deposition, especially for sputtering process. Sputtering are commonly used thin film technologies for the deposition of film with kind of conductor and metals such as Al, Cu, Cr, TiN for circuit logic board, protective carbon coating on magnetic storage head and disks, Chromium are common metal hard coatings. Particulate contamination during plasma deposition and plasma etch process cause vary serious problem during the production of thin films. The problem consist of 2 categories: 1) direct yield loss or scrap the production running parts caused by point defect, 2) reliability problem contributed by film failure rework parts with a lot of cost. Particles were found in RF sputtering deposition processes. [1]

2.2 Physical Vapor Deposition (PVD) sputtering

Sputtering is a physical vapor deposition technique. It requires vacuum conditions and it is used to deposit very thin films on substrates for a wide variety of commercial and scientific purposes. It is performed by applying a high voltage across a low-pressure gas (usually argon at about 5 millitorr) to create plasma, which consists of a quasi-neutral mixture of electron and gas ions in a high energy state. [2] Sputtered films are therefore deposited far from thermal equilibrium, thus metastable phase can be deposited. If a reactive gas (N, O) in introduced into the chamber it is possible to grow a compound film (CrN, Al₂O₃). This is called reactive sputtering.[3] The sputtering process is sometimes called a glow discharge process because the plasma emits a colorful halo of light. Sputtering is a physical vapor deposition (PVD) process involving removing material from solid cathode. This is accomplished by bombardment the cathode with positive ions emitted from inert

This material is reserved for educational use only, not allowed for commercial use.

gas discharge. When ions with high kinetic energy are incident on the cathode, the subsequent collisions knock loose, to sputter atom from target material.[4] The process of transferring momentum from impacting ions to surface atoms forms the basis of sputter coating. The thin film material was deposited by vacuum processes depend on a number of factors. Majority parameter is the energy of the species (add-atoms) incident upon the substrate. Energy range is a few tens of eV for thermal evaporation to tens to hundreds of eV for sputtering. [5]

2.2.1 Ion-surface interactions

During sputtering, energized plasma ions strike a target composed of the desired coating material and caused atoms from that target to be ejected with enough energy to travel to, and bond with, the substrate. When an energetic particle impinge on a surface it transfers momentum to the surface and a number of interactions can take place as can be seen in Figure 2.1 some of these processes cause the desired sputtering of material to the substrate. One thing to keep in mind is that these processes occur both on the target and the substrate.

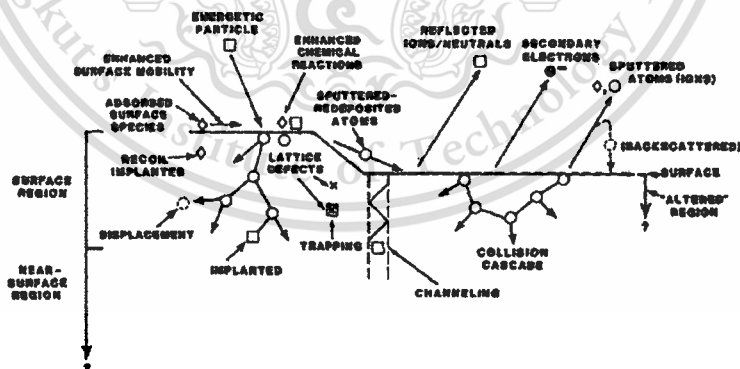


Figure 2.1: Ion-surface interactions.

Probably the most important factor during sputtering is the sputtering yield; the rate which the substrate material is sputtered (sputtered species/impinging specie). This material is reserved for educational use only, not allowed for commercial use.

quantity depends on the incoming ion energy, target material binding energy and the ion and target atomic masses. [6]

2.2.2 Basic plasma physics

The term plasma was introduced in 1929 by Irvin Langmuir to describe the behavior of ionized gases in high current vacuum tubes. It is believed that about 99% of the universe consists of this type of matter. A plasma is a partially or fully ionized gas with properties different from ordinary gases, liquids and solids. The plasma is quasi-neutral, which means that the plasma is neutral averaged over a large volume. This means that the electron and ion densities (n_e and n_i) are most the same. The plasma density (n) is defined as $n = n_e = n_i$. The ionization degree, in plasma given by:

$$\alpha = \frac{n_i}{n_i + n_o} \quad (1)$$

The ratio between the ion density and the sum of the ion and neutral (n_o) densities. When plasma is confined inside a chamber, so called sheaths will be formed around all conducting areas. This can be understood since the electron velocity, V_e , is much larger (>100 times larger) than ion velocity.

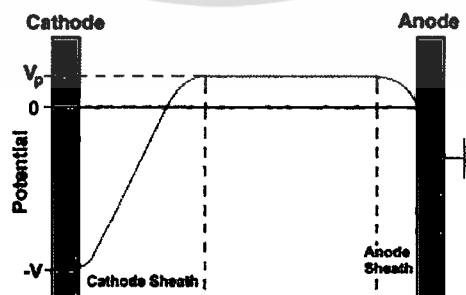


Figure 2.2: The behavior of the potential between two plates, one grounded anode and one cathode at a negative potential, immersed in plasma. V_p is the plasma potential.

Since plasma is simply a region of highly energized gas ions, this is the characteristic "glow" you see during deposition. This plasma "*glow region*" exists just in front of the target surface. Although normally referring to the area at the surface of the target and substrate holder, "*dark space*" is loosely applied to the Faraday Dark Space which occurs between a cathode and plasma in a glow discharge. The dark space tends to confine the plasma to an area that results in active sputtering and any plasma formed outside this area is wasted. Sputtering efficiency is enhanced when the plasma is confined to the region between the target and the substrates. This is accomplished by placing dark space shields on the sides of the target which prevent plasma from developing in areas which do not contribute to deposition.

2.2.3 RF Diode Sputtering

A radio frequency (RF) diode sputtering approach has been developed to sustain a glow capacitive coupled discharge with even electrically insulating targets. A schematic diagram of a RF diode sputter deposition system with plane parallel electrode geometry is shown in **Figure 2.1**. Inert gas (argon) plasma is initiated and maintained between the target and the substrate by the RF power source. In the RF discharge, electrons respond more rapidly to the changing electrical field and tend to flow from the plasma to adjacent conducting surfaces at a faster rate than the ions. Plasma potentials are therefore developed at both the target and the substrate. The positive working gas ions are accelerated across these sheath potentials to strike both the target and the substrate. As a result the plasma can be maintained in a RF diode sputtering approach at considerably lower pressure (5-15 mTorr), than a DC diode sputtering system. Since electrons move along prescribed oscillatory paths behavior in the RF plasma, the loss of electrons from the plasma is also reduced. Because of the high electron-working gas atom collision frequency, the volume ionization efficiency is also high, and the large voltage at the cathode which is essential in a DC glow discharge (for the generation of secondary electrons) is no longer needed for a RF glow discharge to maintain itself. [7]

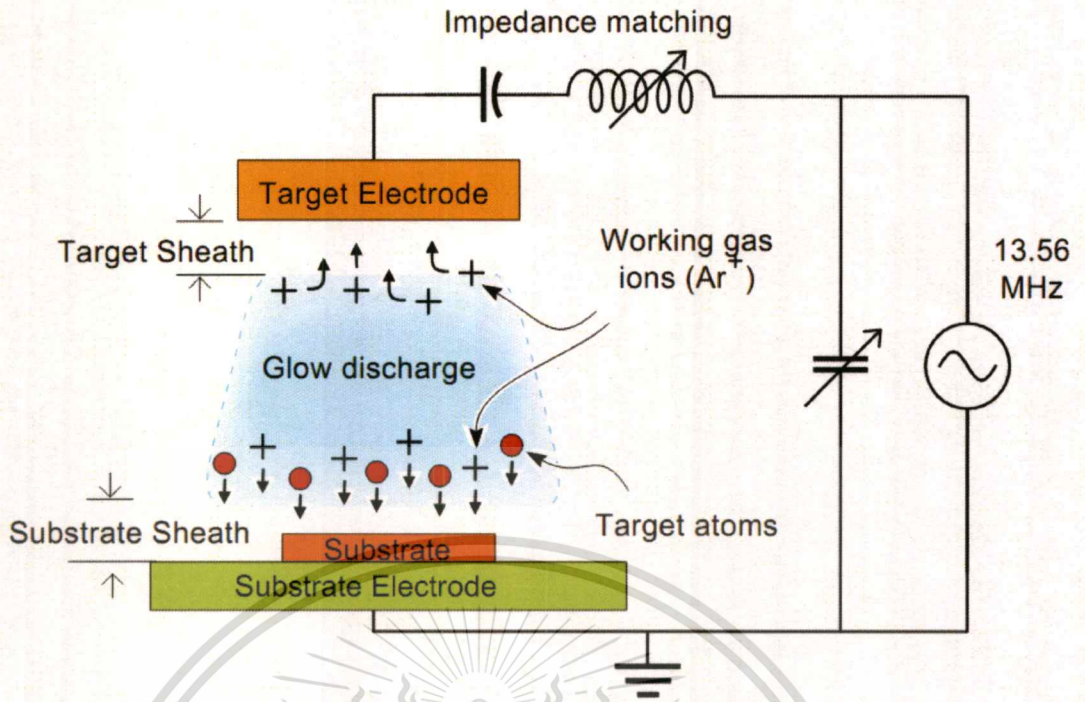


Figure 2.3: schematic illustration of RF Diode Sputter deposition.

The targets plasma sheath potential accelerates positively charged working gas ions towards the target. The resulting energetic ion collisions with the target cause ejection of target atom. These atoms undergo collisions with working gas atoms and they diffuse to the substrate where they condense. Some positive ions also impact the substrate because of a (usually small) substrate sheath potential. [8]

The magnitude of the sheath potentials differ in an asymmetric discharge. The voltage drops across the sheaths are inversely related to the sheath capacitances and thus the substrate and target areas. A bias voltage therefore exists, **Figure 2.4**. As a consequence, one observes that the bombarding ion energy at the typically larger area substrate electrode is less than that at a smaller target electrode. The magnitude of the bias voltage is corresponding to the ion energy at the target. The Argon ions (Ar^+) accelerated across the target sheath bombard the target surface and result in sputtering of metal atoms from the target. These sputtered atoms are then transported to the substrate and deposited. The system geometry, the RF power applied to the plasma and background pressure determines the energies and the fluxes of the ions incident upon the target. These together with

This material is reserved for educational use only, not allowed for commercial use.

the properties of the target determine the energy, angular atoms by working gas atoms during diffusion transport to the substrate modifies these quantities. The final energy and angular distributions of the metal atoms incident upon the substrate therefore depend on the target to substrate distance, the working gas type, and background pressure. Working gas ions are also accelerated across the substrate sheath and strike the substrate with the energies in the 40-140 eV range. The energy and flux of both the metal and argon ions as they strike the substrate can have potentially important effects upon the resulting film properties. The film microstructure gives a graphic representative of how changing process pressure and wafer temperature affects the structure of a PVD film. [9, 10, 11, 12, 13, 14, 15, 16]

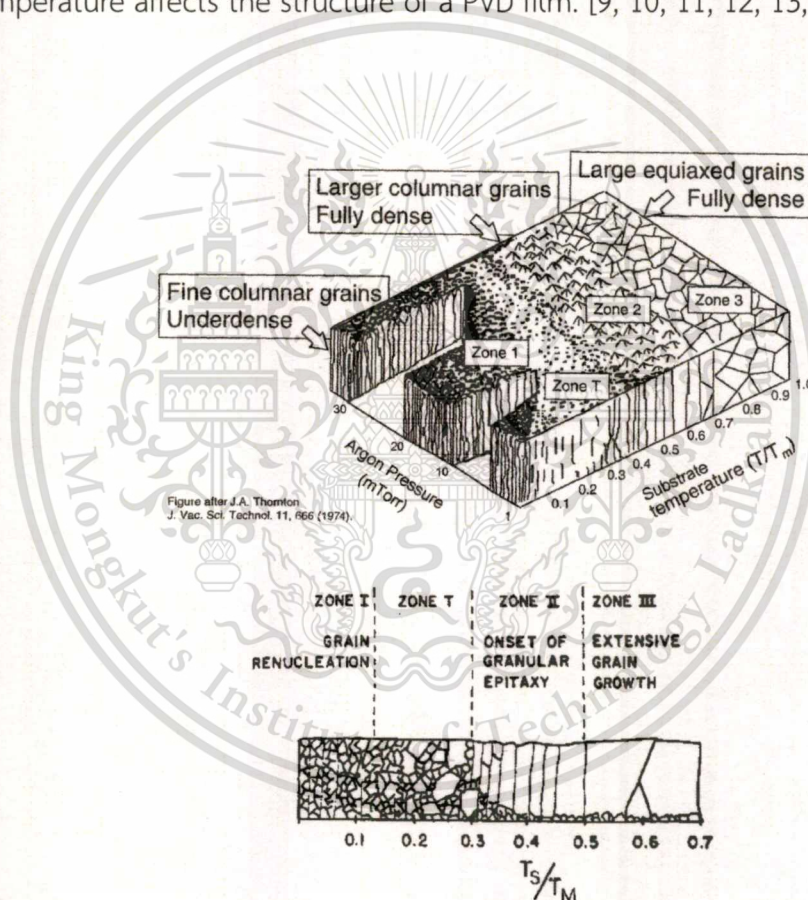


Figure 2.4: Dependence of the sputtering yield of several elements (ordered according to their position in the periodic table) calculated using SRIM (initial conditions: 300eV Ar, other input parameters where set at the standard values given by Stopping and Range of Ions in Matter (SRIM): lattice binding energy, surface binding energy displacement energy, and normal incidence).

2.2.4 Sputtering mechanics

Sputtering is a method of coating material onto a surface substrate. This is accomplished by using physical vapor deposition (PVD). If a solid material has energy applied to it, the atoms begin to vibrate faster and faster, until the atoms have enough energy to cause the release of electrons from the outer shell. The distance between molecules move faster and faster until strike one another with sufficient force to cause electrons to be knocked off. This loss leaves the molecule with a positive charge. The positive charge molecule is called a positive ion. And the process of losing an electron is called ionization. In sputtering target and substrate, plates are housed within a chamber which has most gases removed creating a vacuum. The chamber is then filled with inert gas (non-reactive), typically argon, to supply a medium from which ions can be made. The target plate is used as a source of solid material to be knocked off and coated onto an adjacent surface or substrate.

RF diode sputtering used on Alcatel 2460 machine. Radio frequency (RF) is applied as the energy source to excite the molecules at the proper time, rate, and sequence to create a electrical charge used to control the movement of the molecules. (The excited ions create a glow as electrons re-combine with positive ions. This is called plasma.) The impact of the ions hitting the target erodes the surface material. This erosion is called sputtering. Since the chamber is maintained at low pressure, few other atoms (molecules) interfere (scatter) the target material on its way to the substrate. Under the right conditions, the sputtered target material collects on the substrate as a thin growing film. Plasma is an excited gas which consists of atoms, molecules, ions, free radicals, free electrons, and metastable species. The chemistry of plasma is complex because many different interactions are possible: electron-atom/molecule, electron-metastable atom/molecule, ion-atom/molecule, etc. If the molecular structure of the gas is not particularly simple, the chemistry of the discharge is very complicated and depends on plasma parameter. [3, 17, 18]

2.2.5 Description of plasma

Different types of plasma can be created, depending on experiment conditions. The most frequently cited types are thermal plasma, corona or point-plane discharges, and cold plasma. Thermal plasmas or hot plasmas are obtained by coupling energy into a high pressure gas, normally using DC current, AC current, radio frequency (RF), or microwave (mw) in thermal plasmas. A temperature of some thousand degrees centigrade is reached by coupling electromagnetic energy into a high-pressure gas under equilibrium condition. One of the effects is the cleavage of many chemical bonds, with formation of very reactive species, which can either form new compounds or interact with surfaces. Typical application of this type of plasma is synthesis of ceramic powders and the deposition of ceramic coatings. [19, 20]

Corona discharge can be sustained at high-pressure gas using the physical fact that close to a conductor with a small radius of curvature, the electric field is much higher than when it is flat. A typical apparatus for corona discharges is shown in **Figure 2.5**. Thin wires are held at high voltage respect to ground. Films are rolled around a grounded cylinder and pass through the discharge, where it is expected that their surface will be activated. Corona systems are very common in the plastic film industry for the activation of polymer surfaces. [21, 22, 23, 24, 25]

Corona discharge point attachment for electrophorus

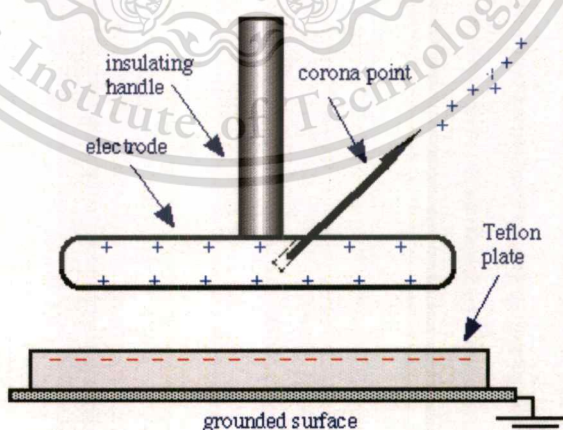


Figure 2.5: Corona discharge point attachment for electrophorus.

Glow discharges or cold plasmas are excited again by DC, AC, RF or mw but operated in gases held at low pressure and temperature as **Figure 2.6**. It is easier to
 This material is reserved for educational use only, not allowed for commercial use.

control than corona, and it is rather flexible. The main distinction encountered in cold plasma treatments is between etching and deposition. The effect of the treatment is normally evaluated in terms of loss or gain of weight. [26, 27, 28]

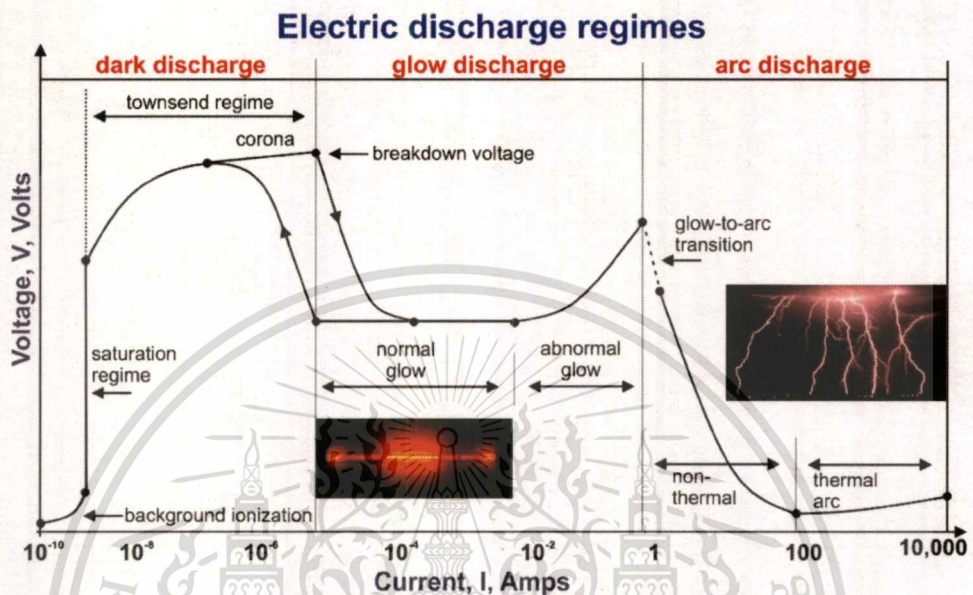


Figure 2.6: A typical V/I plot of a glow discharge. The main characteristics of the discharge, the voltage current characteristic and the structure of the discharge depend on geometry of the electrode, the gas used, the pressure and the electrode material.

2.2.6 RF diode sputtering equipment

Sputtering equipment usually consists of power supply, vacuum system, reactor chamber, matching network, power monitor, and control system. The energy used to create the plasma is ac current. The conventional frequency for RF is 13.56 MHz and it has two divided inductive coupling and capacitive coupling. The vacuum chamber is able to reach desired pressure, typically in the $1\text{-}10^{-7}$ torr range. And the vacuum chamber is metallic, stainless or aluminum being flow meters in applications such as thin film coating. There are 7 main parameters is used in the operation of a glow discharge for sputter deposition of thin film. [29] They include:

2.2.6.1 Pressure

As the background gas pressure is increased, the discharge current increase, the applied voltage falls, the number of working gas ions increase but their energies decreases. Since the sputter yield increases with the number of ions and ion energy, the total number of atoms ejected from the target will depend on the base pressure. When the pressure is low, the mean free path between collision is large compared to the sputtered atom to substrate distance. At higher pressures, sputtered atoms suffer more collisions and are thus prevented from reaching the substrate. [30]

2.2.6.2 Deposition distribution

Under high pressure, because of collision with the working gas atoms, the sputtered atoms are diffusely scattered during transit and therefore reach the substrate with certain directions and energies. As a result of diffuse nature of material transport, the atoms at high pressure deposit at place not necessarily in the line of sight of the target.

2.2.6.3 Power

The sputtering rate is proportional to the ion current incident on the target. For a constant voltage, it is therefore proportional to the input power which is thus a key control parameter. In most of RF diode sputtering system, the ion impact current and voltage are in phase.

2.2.6.4 Cathode

In order to obtain a uniform deposition thickness, the area of cathode (target) must be much larger than the area of anode (substrate) and the separation distance must be a small fraction of anode diameter. The cathode materials may be in the form of a plate, cylinder, or foil, and can be electroplated onto a suitable target support material. Because of intense ion bombardment, the cathode gets hot. The temperature usually increases rapidly and finally will approach to an equilibrium value. Both the rate of temperature rise and the maximum temperature attained depend on the power dissipated at the cathode, the thermal characteristics (such as

conductivity and emissivity) of the target, cooling system capacity, the gas pressure etc. [7]

2.2.6.5 Contamination

Even if a sputtering system is initially pumped down to a low pressure and then a sputtering gas of high purity is admitted, contamination may still result from outgassing as a result of plasma-discharge heating of chamber walls. Other contaminations are found as a result of decomposition of oil vapors due to back streaming from diffusion pumps.

2.2.6.6 Deposition control

One of the chief advantages of the sputtering technique is that the rate of deposition remains constant with time, provided the current density and voltage do not vary a condition that is easily attained by using an automatic pressure controller and a regular power supply. It is important to position the monitor so that it does not disturb the plasma. Substrate is coated with 3 steps on Comtech 2460 machine. Firstly, Pre clean substrate step. Substrate is cleaned by using argon ion plasma. The shutter still closes during clean substrate surface. Secondly, Pre sputtering step. Target is sputtered remove any contamination and target surface before coat chromium film on the substrate then shutter is opened. Finally, Substrate has move down close to the target with distance 1.6 centimeter as show schematic **Figure 2.7**

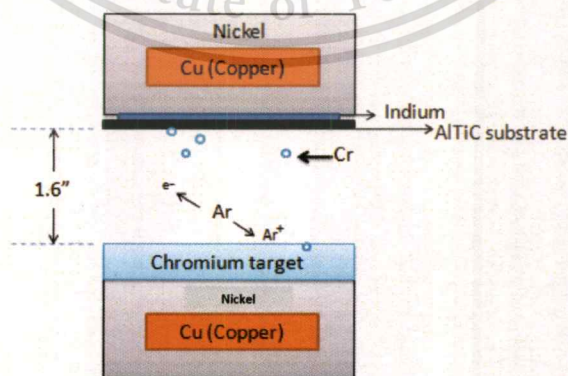


Figure 2.7: RF diode sputter deposition system consists of a vacuum chamber, a sputter source, vacuum sensors, a substrate holder, and pumping system.

These systems have the constant flow of Argon gas into the chamber. Deposit pressure is controlled by the rate of gas passing into the chamber and by a throttle valve placed between the vacuum pump and deposit chamber. Throttle valve control the pumping speed which have the gas flow into the system, a constant pressure of deposition approximately 0.1-100 millitorr (mT) is maintained. This supply of gas is ionized using large potentials at the source to become generation of plasma. After that plasma sputter from a target material to the substrate and the chamber walls.

2.2.6.7 Sputter source

The two most common types of sputter source are diodes and magnetrons. Both of all configurations can be operated with direct current (DC) or radio frequency (RF) potential to generation plasma through the ionization of inert gas. Diode sputter source consists of target in the shape of a flat disk or rectangular target solid material bonded to wafer cooled plate. An external potential is applied from outside power source, charging the target to a high negative voltage (3-5kV). Ar gas is introduced into the vacuum chamber between target and the grounded substrate and chamber walls. The large difference in potential from a plasma, caused by ionization of the Ar atom in the electric field. The ionization results are a negatively charge electron and positively charged ion pair, where as the plasma itself retains a net neutral charge. Positively charged ions are attracted to the negatively charged target to accelerate by electric field. Bombardment of the target with these high energy ions lead to sputtering of the target atoms. Forming and coating on the substrate. In this type of configuration, the target substrate holder and ground vacuum used can be considered a parallel plate capacitor.

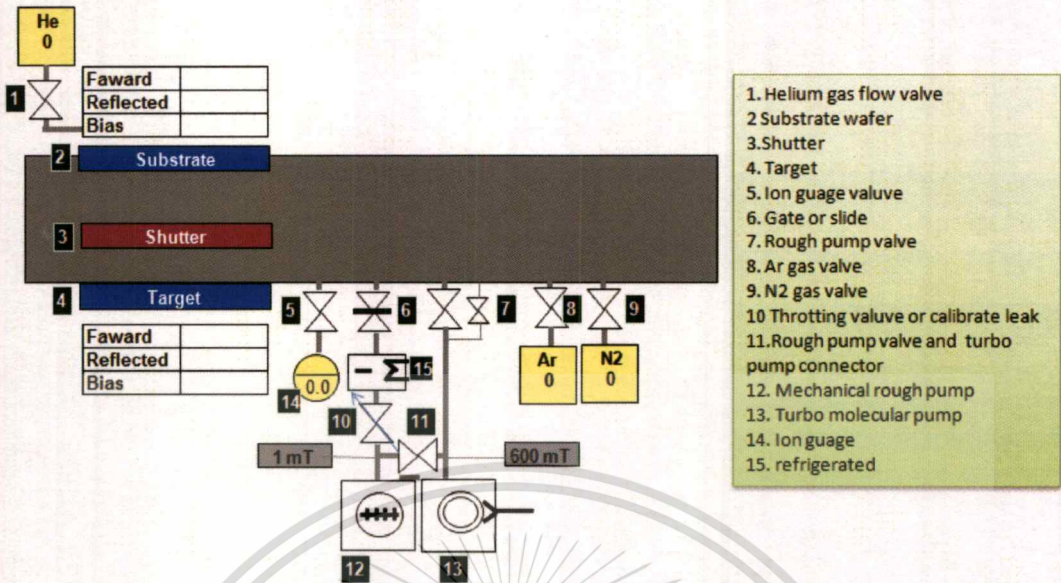


Figure 2.8: Schematic of Comteh coating machine.

The significance of metal ionization rates can be described as follows the energy during the deposition, Contamination also generates depend on the atomic masses has a columnar structure and a smooth coating surface without of presence of macro particle. In micro structure, Energy metal ions during ion bombardment knock of some metal atoms from within the substrate and may be penetrate the substrate lattice to angstrom levels. Defects could be generated on the substrate atomic level.

2.2.6.8 Mechanical properties of Chromium films

Chromium film properties are extremely sensitive to deposition conditions. The preferred orientations of Cr films are body center cubic (BCC) structure with BCC 110 or BCC 200 or both depending on Ar pressure [9]. Chromium materials have high wear resistance, good corrosion resistance and low friction coefficient [10]. Currently, Many industrials have select chromium for using in coating system such as solar cell application support light energy absorber, use in photolithography mask application and digital magnetic recording.

Table 2.1 Material Temperature for given vapor pressure.

Temperature (°C) for given vapor pressure (Torr)							
Material	MP(°C)	g/cm ³	10 ⁻⁸	10 ⁻⁶	10 ⁻⁴	Sputter	Comment
Chromium	1857	7.2	837	977	1157	DC,RF	Film very adherent
Copper	1083	8.92	787	857	1017	DC,RF	Poor adhesion, use adhesion layer of chromium
Gold	1064	19.32	807	947	1132	DC,RF	Poor adhesion

2.2.6.9 Hardness and Elastic modulus

The reduced elastic modulus, E_r of a deposited coating can be determined by nano-indentation techniques with the following equation:

$$E_r = \frac{\sqrt{\pi} S}{2 A} \quad (2.2)$$

Where S is the stiffness of the specimen, A is projected contact area of indentation. The elastic modulus of the test material, E , can be determine from

$$\frac{1}{E_r} = \frac{1-\nu^2}{E} + \frac{1-\nu_i^2}{E_i} \quad (2.3)$$

Where E , ν , E_i and ν_i are elastic modulus and Poison's ratio of the test specimen and indenter respectively.

An indenter tip is driven into the sample surface by applying an increasing load up to a predefined value. The load is then decreased until partial or complete relaxation of the material occurs. Data reported in this study is based on a type of indenter with an applied force to achieve a penetration of less than 10% of coating thickness.

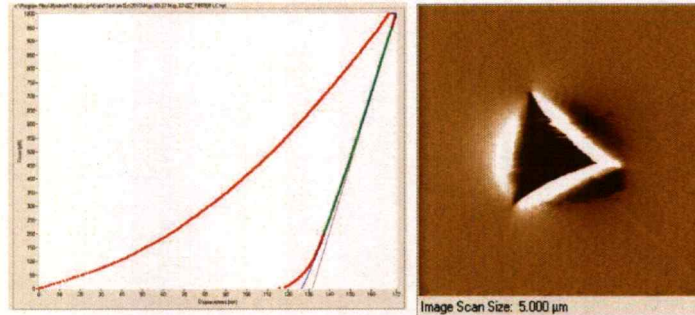


Figure 2.9: Force versus displacement curve on film showing typical response of elastic-material and resulting in-situ SPM image of surface after quasi-static indentation showing residue indentation impression.

2.3 Characterization of Cr film

2.3.1 Scanning electron microscope (SEM)

SEM was used to observe the surface morphology of Cr films operated at 5 kV image viewed 20,000X and 50,000X magnification. The wide variety detectors available for the SEM can be classified into two types: those sensitive to backscattered electrons and secondary electrons. Secondary electrons mode has closed surface film identify. In this study, the characteristics of Cr samples have been studied according to the deposit pressure, substrate bias voltage using scanning electron microscopy (SEM) with EDX mode to observed type of contamination on chromium surface. Capture grain size image morphology was investigated the influence of the substrate bias voltage, deposit pressure.

2.3.2 Atomic force microscopy (AFM)

Surface topography of chromium film was investigated intensively by atomic force microscope. The sample needs not electrically conducting and sample preparation is relatively simple. It is also possible to obtain surface information similar to that provided by scanning electron, but better sensitivity to surface corrugation. The digitized image data of AFM have more advantages than image of SEM because they can be analyzed easily by surface analysis software to measure surface roughness and its fractal dimension. The range of magnification covers that for th optical microscope (microns) to that for the electron microscope (Angstroms).

The AFM records forces between the apex of a tip and atoms in a sample as the tip is scanned over the surface of the sample. The AFM system is shown in **Figure 2.10**

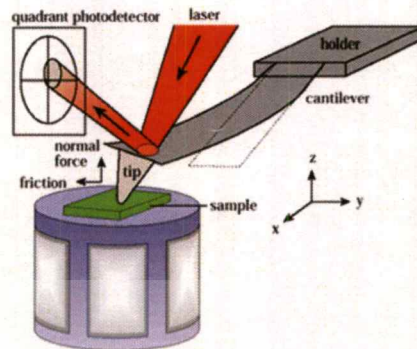


Figure 2.10: AFM detect the sample by using cantilever.

The AFM system consists of a sample positioning system and electronic control unit, microcomputer with a super VGA color monitor, an optical microscope connected to a monochrome monitor, and a vibration isolation system in a fully integrated system. Since vibrations cause unwanted motions of the probe tip relative to the system, they yield a substantial decrease in resolution. Therefore a vibration isolation system is crucial for AFM studies. The initial tip-approach to the sample was facilitated by an optical microscope which provided a 45° view of tip and sample with magnification from 100X to 300X. The tip can be made of a small fractured diamond fragment attached to the cantilever spring or an integrated silicon nitride tip. The scanner in this study is the 70-micron scanner. The mode of operation is constant force mode. In this mode, the force on the cantilever is fixed while the sample is scanned. The voltage applied to the vertical piezoelectric translator to maintain a constant cantilever deflection (force) provides the image signal. The constant force mode requires high responsiveness of the feedback electronics, so it is used to scan large areas (typically larger than $100 \text{ \AA} \times 100 \text{ \AA}$) and large surface features.

After the tip-approach was performed, the line scan mode was selected in order to diagnose the feedback response to the surface features. In this mode, the scanner moves the probe repeatedly over the first scan line to test the control value and scan speed can be adjusted by operator. Good feedback loops respond to the surface features indicated by overlapping lines seen in the voltage and current traces. The force used at the cantilever was set as light as possible so as to not damage the sample, but sensor sense atomic force accurately scanned. The scan

This material is reserved for educational use only, not allowed for commercial use.

rate was controlled to be 2 Hz for low magnification images. A resolution of 300x300 data points per image was used to collect the data. On the roughness area, There are two surface roughness parameters which are frequently used, i.e., average roughness (R_a) and root-mean-square roughness (RMS). The R_a is the arithmetic mean of the absolute values of departures of the roughness profile from the mean line. For N measurements of height Z, R_a can be written as:

$$R_z = \frac{1}{N} \sum_{i=1}^N |Z_i - \bar{Z}| \quad (2.4)$$

The root-mean-square roughness is the standard deviation of the height measurement which can be written as:

$$R_{ns} = \sqrt{\frac{1}{N} \sum_{i=1}^N (Z_i - \bar{Z})^2} \quad (2.5)$$

2.4 Thickness non-uniformity measurement

To evaluate the uniformities, we measured thickness of chromium film total nine points on the wafer by using micro-head Tencorr machine. A universal equation widely used in the industry show in equation (2.6), where H_{max} and H_{min} denote the maximum and minimum thickness within measured the sample,

$$\% Non - uniformity = \left[\frac{H_{max} - H_{min}}{H_{max} + H_{min}} \right] \times 100 \quad (2.6)$$

2.5 Laser techniques

The host of laser measurement techniques, Laser Induced Fluorescence (LIF) and Cavity Ring-down Spectroscopy (CRDS) are among the most common. To detect particles with a laser, one must first identify a useful transition wavelength. Since most particles have different spectral lines, a different laser is typically needed for each material of interest, which can rapidly become very expensive. However, once a spectral line is selected, laser measurements can detect part-per-billion to part-per-trillion quantities of particles, giving them orders of magnitude higher sensitivity than most other methods to detect particulate contamination. Once a spectral line has

This material is reserved for educational use only, not allowed for commercial use.

Forbidden to modify the content, and cite the document when use.

been selected and an appropriate laser chosen, there are two fundamental ways to detect the particles themselves. First is LIF, the laser is injected into the path of the sputtered particles. When a particle passes through the beam, it absorbs a photon and reaches an excited state. Particles which do not share the spectral line pass through the beam to no effect. Once the sputtered particle has been excited, it very quickly releases a photon to return to the ground state. A very sensitive detector such as a photomultiplier tube is then used to detect the released photons, giving a particle count. In vacuum, typically the quality of the detector is the limiting factor for particle detection. At higher pressures, scattering rapidly becomes of greater significance. Larger sputter yields also mean stronger signals, and conversely, smaller sputter yields result in weaker signals, making high-quality detectors even more important in laser sputter detection.

With CRDS, the chosen laser is injected into a cavity formed by two high-reflectivity mirrors (>99.9%). **Figure 2.11** CRDS schematic. The laser beam reflects tens of thousands of times between the mirrors before eventually decaying to zero, effectively increasing the path length that the laser travels through by several orders of magnitude. When the cavity is empty (i.e. in vacuum), the light decays with a time constant τ_0 . This decay is called a “ring-down”. When the target particles (called “absorbers”) are present in the cavity, the decay rate is accelerated because some of the light is absorbed during each reflection. This generates a new decay time constant τ , which can be compared to the empty cavity time constant to generate a particle number density in the cavity. It is important to note that neither method presented here can provide information on the emission direction of the sputter products, only the total number emitted.

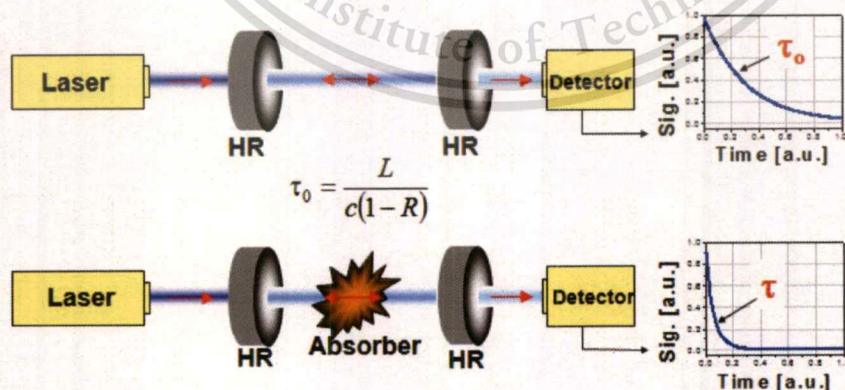


Figure 2.11: CRDS schematic laser particle count.

2.6 Literature reviews

Chromium film issued hardmask coating. Film surface properties are key factors to do hardmask patterning process. Chromium film thanks to thermal stability, high wears resistance, and good adhesive layer for lithography process given sharp pattern edge on lift-off process and smooth surface. Many coating parameter modifications have been attempted on chromium films to improve stripped process, patterning surface defect on the specimen such as wafer coating lithography process, annealing film given good film properties. Film hardness roughness and grain size of the film.

Miguel et al.[9] studied corrosion resistance of steel. Morphology and corrosion of chromate coating was studied with difference substrate. The difference in corrosion protection was observed by polarization curve. Growth film of different substrate was attributed to the structure properties thickness coating, grain size and roughness observed.

Martin and Friedrich [10] studied coating material for different physical vapor deposition (PVD) techniques. These studies focus on solid coating and sputtering material such as TiO_2 , SiC , ZrO_2 , MgO . The requirements of these materials are discussed properties listed and production.

Shtereva et al. [11] studied thin films by RF diode sputtering for solar and optoelectronic applications. Nitrogen was investigated as a functional of the nitrogen content in the sputtering gas. ZnO:N thin films prepared by RF diode sputtering and using N_2 source as a dopant. The energy bombards substrate as well as substrate temperature has a significant influence on properties of ZnO film.

Balu and Raju et al.[12] investigated the process parameter on the structural of ion beam sputter deposited chromium thin films. The structural variation and morphological variations observed have been discuss based on the Silicon (100) growth models and the energetic involved in the process. The structure transform from (100) orientation to (200) orientation.

Adlbi et al. [14] studied the effect of parameter ion energy during deposition on the microstructure and crystal orientation of deposited film. In this case of reactive

sputtering, the concluded that a variation in surface chemistry due to biasing which affects surface energy leads to a specific preferred crystal orientation.



Chapter 3

Experimental details

3.1 Materials

3.1.1 Chromium target

Chromium target was provided with rectangular shape The Chromium target was 99.95% wt. % in purity diameter 17"x17" from AVP co., ltd

3.1.2 ALTiC substrate

ALTiC substrate was prepared circular shape 6 inches diameter wafers.

3.1.3 Gas

Argon gases 99.995% in purity and Nitrogen gas 99.999% in purity which Argon gas was prepared sputter gas and Nitrogen provide reactive gas.

3.1.4 The background deposit pressure

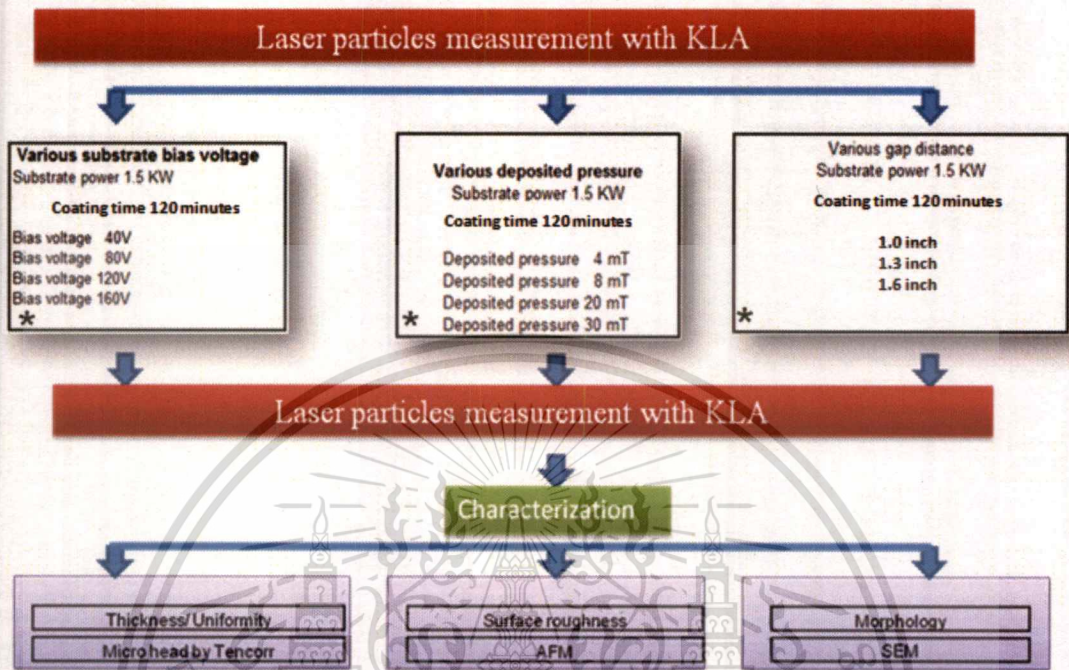
The background deposit pressure was 2×10^{-6} Torr.

3.2 Instruments

Table 3.1 List of instruments and their manufactures

Instruments	Manufacturers
Sputtering vacuum system	Comtech 2480 model
Atomic Force Microscope	XE-PTR
Wafer cleaning	SSEC model 3300
(Scanning electron microscope) SEM	PTM600
Wafer cleanliness laser visual inspection	KLA
Micro-head thickness measurement	Tencorr
Nano-indenter	Hysitron

3.3 Flow chart of the experiments



The Alcatel Comptech 2460 dielectric RF sputtering system was utilized for this research, as shown in Figure 3.1. In parallel plate system, two electrodes, one being coupled to an RF power generator, the other being grounded, are used to create an electrical field between the electrodes. A vacuum chamber size is 30"width x 60" length x3.5" height and fabricated from non-magnetic type 304 stainless steel. Inside the vacuum chamber is a shutter assembly consisting of an aluminum flat plate which can be positioned between a target holder and a substrate holder during pre-sputtering and pre-clean processing.

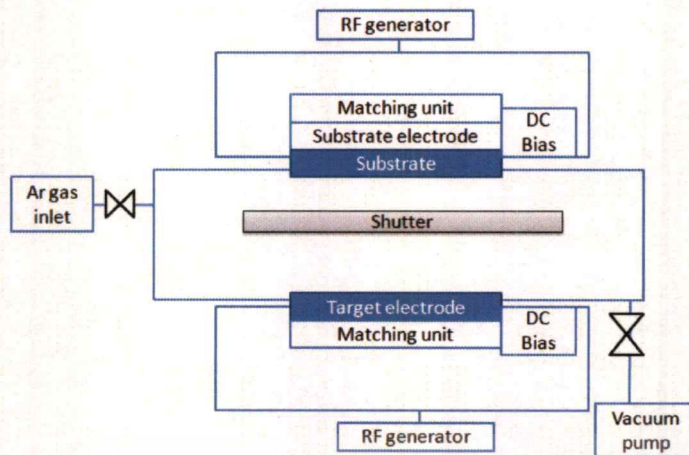


Figure 3.1: Schematic of Alcatel Comptech 2460 RF sputtering.

The target and substrates were loaded face up onto a square 17" x 17" nickel plated oxygen-free high thermal conductivity (OFHC) copper substrate holder. The substrates held in place by retaining stainless steel 304 screw and alumina (Al_2O_3) button. The substrate loading capacity is 4 wafers for a cycle. The substrate holder was placing 1.6" above the target. The target was made of chromium purity 99.5% with a dimension of 17"x17". Aluminum titanium carbide (ALTiC) round wafer 6" diameter and 1.2 millimeters thick was used as the substrate.

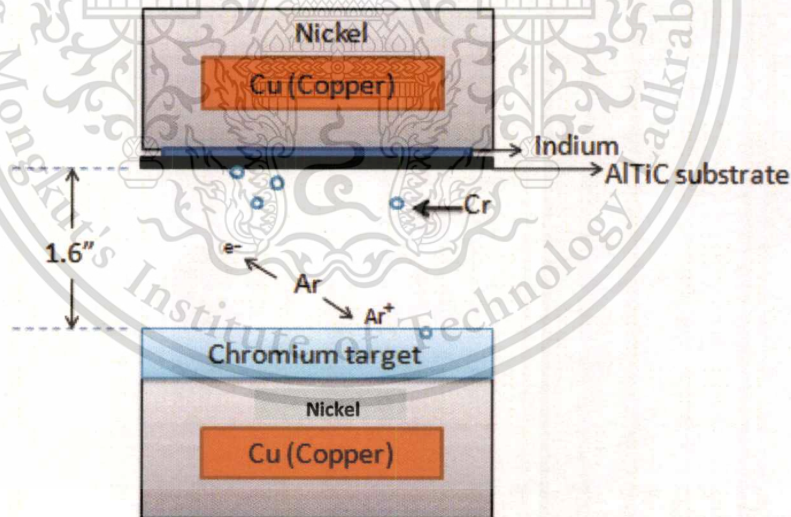


Figure 3.2: Schematic of target and substrate electrode.

3.4 Sample preparation

3.4.1 ALTiC substrate

ALTiC was prepared by nylon brush cleaning on the substrate. DI water and IPA used to remove contamination such as particle lubricants then dried in vacuum moisture release at 7×10^{-2} Torr total 5 minutes. The substrate positions in a

sputtering chamber were also investigated. The Alcatel Comptech 2460 dielectric RF sputtering system was designed to load 4 substrates per run. It was also designed Ar gas inlet near the substrate wafer at position no.1. Vacuum pump system link to the sputtering chamber, Vent out be at between substrate wafer no.3 and no.4, as shown in **Figure 3.3**. Moreover, the contaminations before coating were not overlooking. Since substrates have cleaned before coating till reach acceptable level of contamination. The particulate contamination after coating observed from the KLA machine was expected to generate from sputtering environment. The correlation of contamination before and after coating was considered.

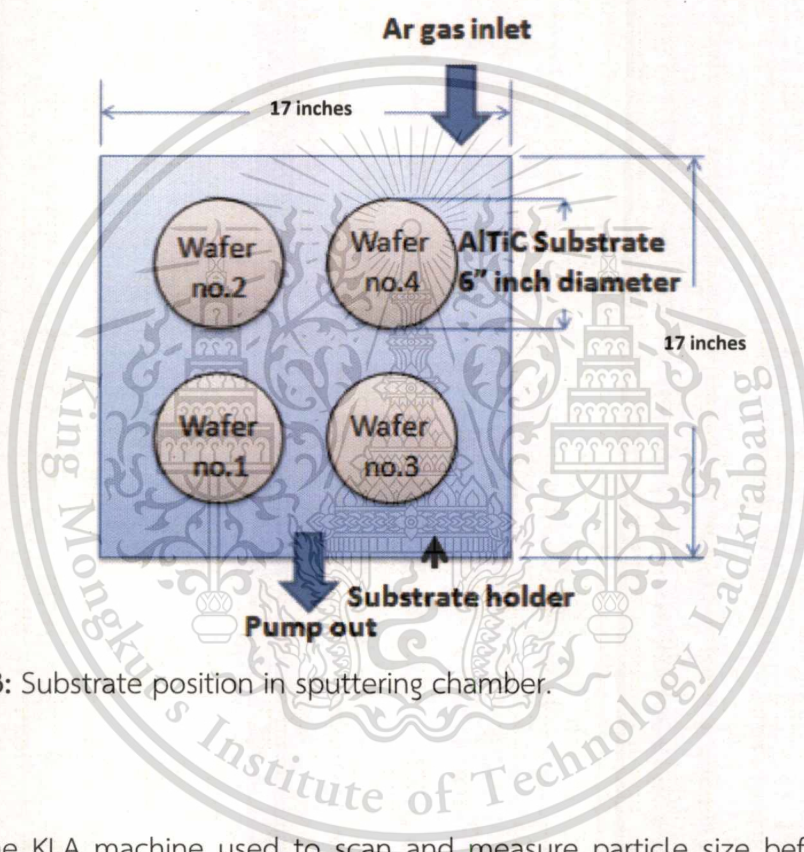


Figure 3.3: Substrate position in sputtering chamber.

The KLA machine used to scan and measure particle size before and after coating. The KLA scanning particle was done outside sputtering chamber. A light source is laser with wavelength of 633 nm. Laser spot size is approximately 5 μm . The substrates were put on permaluk state and held in place by vacuum system. State was set to rotate 3200 rpm during scanning. Because of rotating 3200 rpm, dust or particles outside chamber that may fall on the film surface after finishing coating are negligible since they will be blow away during scanning. The size of particulate contamination less than 3 μm is negligible because, the minimum particle size that KLA can detect is equal or larger than 3 μm .

To identify the source of contamination, the particulate contamination on the chromium film surface was characterized by FE-SEM with EDX. The Alcatel Comptech

2460 dielectric RF sputtering has not real time thickness measurement system because there is no Ellipsometry inside the chamber. Then all recipe were set sputtering time at 120 minutes. The sputtering conditions were varied only interested parameter but fix other parameters. The experiment was divided into 3 groups. Group 1 varied processing deposit pressure while other parameters were controlled. Group 2 varies substrate bias voltage and group 3 varies distance between 2 electrodes, other parameters were controlled also. In this studied, AFM was used for roughness measurement. The average roughness (R_a) and root mean square roughness (R_{RMS}) were calculated from digitized image data using the topography surface analysis software. First, each image was flattened by using second order leveling to reduce the effect of chromium film curvature on the roughness measurement. Then, AFM images for $5\ \mu\text{m} \times 5\ \mu\text{m}$ scanning areas were used to study the roughness of each chromium film surface measurement.

3.4.2 Typical vacuum deposition system

The five basic parts of a vacuum system consist of the deposition chamber, associated substrate fixture, vacuum pumping system, the exhaust system and the processing gas system. The system is first roughed down with the mechanical pump. The rough valve is then closed and the high vacuum valve is opened which allows the pumping system to pump down and evacuate the chamber to a base pressure. The time it takes to get to a specific base pressure is a very important operational parameter. After attaining the desired base pressure, the high-vacuum valve may be closed and the time for the system to rise one decade in pressure can be noted. This leak-up rate is an indication of the gas and vapor sources in the chamber. The time-to-base pressure and leak-up rate are indications of the condition of the vacuum system and changes in these values may indicate a system problem or that the system needs cleaning. Mechanical or rotary oil-sealed pumps are also referred to as roughing, backing, fore or holding pumps, dependent upon how they are being utilized. They can be connected directly to a vacuum system and discharge into the atmosphere or be used as a backing pump for another type of pump. Generally speaking, the ultimate pressure of oil-sealed rotary pumps is limited by the vapor pressure of the oil and leakage of air past the seal between exhaust and inlet ports. All oil-sealed pumps have an oil reservoir because the oil film is used as a seal on the valve seat. Reservoir capacity is determined by actual pump speed and maintenance, service requirements. In most cases the operating temperature of the oil is 50°C to aid in boiling off contaminating liquids and gases. When the oil in a mechanical pump becomes contaminated, it should be drained and replaced with

This material is reserved for educational use only, not allowed for commercial use.

new oil. In the early stages of the evacuation process, the ejected air will contain a large amount of oil mist. Therefore, the ejected air is exhausted through a mist eliminator which is similar to an automobile carburetor air cleaner.

3.4.3 Step of chromium film hard coating by RF diode sputtering

For this topic explain step of vacuum process and parameter controlled during process step of Comtech machine. The step consist 3 portions. Sputter – etch Pre-sputter and Deposit. In order to ensure plasma is struck at the typical system operating pressures, a separate source of ignition is used. This ignition source consists of a high voltage transformer located on the top of the chamber (left hand side), and an electrode inside the process chamber. The output of the transformer is connected to the electrode by way of a vacuum feed through. This electrode is in close proximity to the target and substrate holder. When the system is ready to strike a plasma (gas flow and chamber pressure are stabilized), the RF generator is turned on and 110 volts AC is applied to the primary of the igniter. This results in an output of 10 kV from the secondary. This voltage is applied between the electrode and chamber ground creating an arc which ignites the plasma. The igniter is controlled automatically by the PLC in both automatic and manual modes. When a process step is selected (sputter-etch, pre-sputter, deposit) the PLC engages the igniter. There are two standard pumping packages available with the system and various optional pumps. The pumping system consists of a primary pump and a secondary pump. The mechanical pump is used in two situations.

The primary pump is used to reduce the process chamber pressure to below 10^{-1} Torr (crossover point) at which point the high vacuum pump can take over. The secondary pump then reduces the chamber pressure to a user defined at set point (typically less than 10^{-6} Torr). On systems with a mechanical pump, the pump is connected to the system by way of a molecular sieve trap located at the pump intake. This trap contains material (Zeolite) which adsorbs mechanical pump oil vapor minimizing the possibility of oil vapor back-streaming into the chamber or turbo pump. This molecular sieve trap contains a heater element which, when energized, will vaporize trapped material which is then pumped out through the mechanical pump. ALTiC substrate wafer were pump down to be vacuum on the substrate holder (Backside of wafers). Helium gas was flow for cooling ALTiC substrate wafers before start process procedure setup as shown **Figure 3.4**.

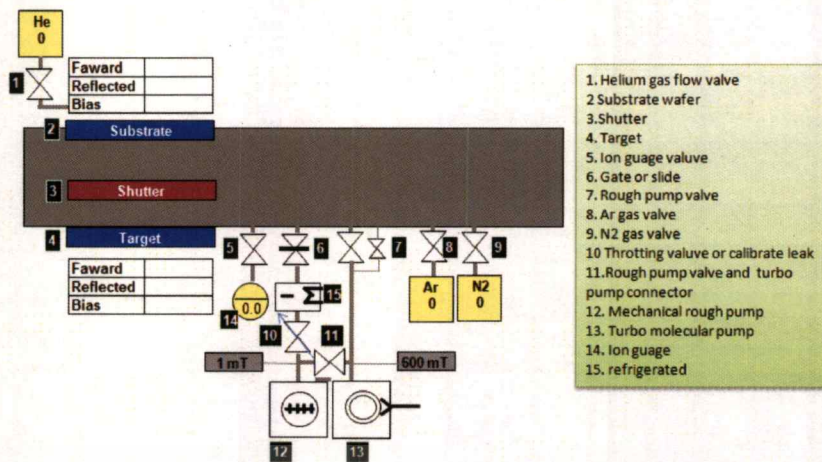


Figure 3.4: The working area contains screen views depicting the system.

3.4.4 Sputter-etch step

When the system is opened for loading or unloading, the substrate holder is replaced with a pre-loaded holder or the substrates are individually loaded and unloaded. This substrate holder and the substrates contain absorbed gases and water vapor from being exposed to atmosphere. Pumping the system down to a high vacuum will remove most of the absorbed gases, but again, not all. To minimize the possibility of sputtering onto a contaminated substrate surface, substrate cleaning is performed prior to depositing ALTIC wafer substrate. This process step is called sputter-etch (substrate pre-clean). This step is normally run first step and the shutter is still positioned between the target and the substrates. In sputter-etch, the system is run in a deposition mode except the substrate is operated as a target and the shutter becomes the surface deposited upon. When RF is applied to the substrate holder, argon ions collide with the substrates, and erode material from them, which is deposited on the shutter. This removes any contamination from the substrate surface and also removes a thin layer of the substrate material itself resulting in a better surface to deposit upon (adhesion). Material deposited on the top of the shutter must also be periodically removed or the shutter replaced as a normal maintenance procedure. Again, the chamber wall tends to be scrubbed by the active plasma, further reducing the contaminant levels. The first step is pre-etch step, roughing valve (no.6), Backing valve (no.10) and plate valve were closed. The machine switch on system with flow Argon gas into chamber (no.8 turn on) mechanical rough pump start to pump down from atmosphere to 10^{-2} mT after that Thermo pump was pump down from 10^{-2} mT to 10^{-6} mT. (plate valve is opened)

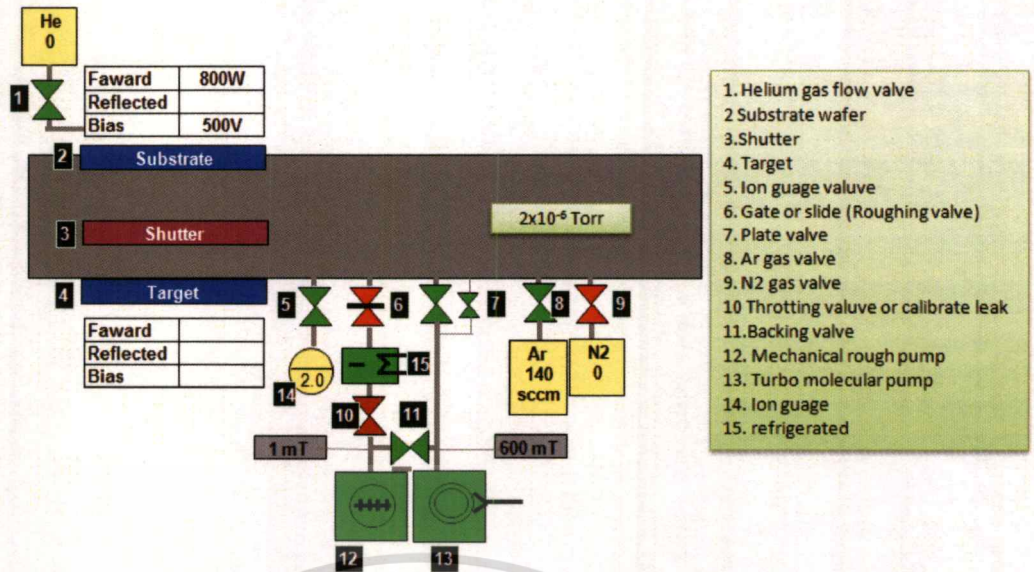


Figure 3.5: Vacuum system diagram when the system pumps down to base pressure.

When the system meet target base pressure 10^{-6} Torr Ar gas valve was open for generate plasma and vacuum chamber following set point 8mT as shown Figure 3.6

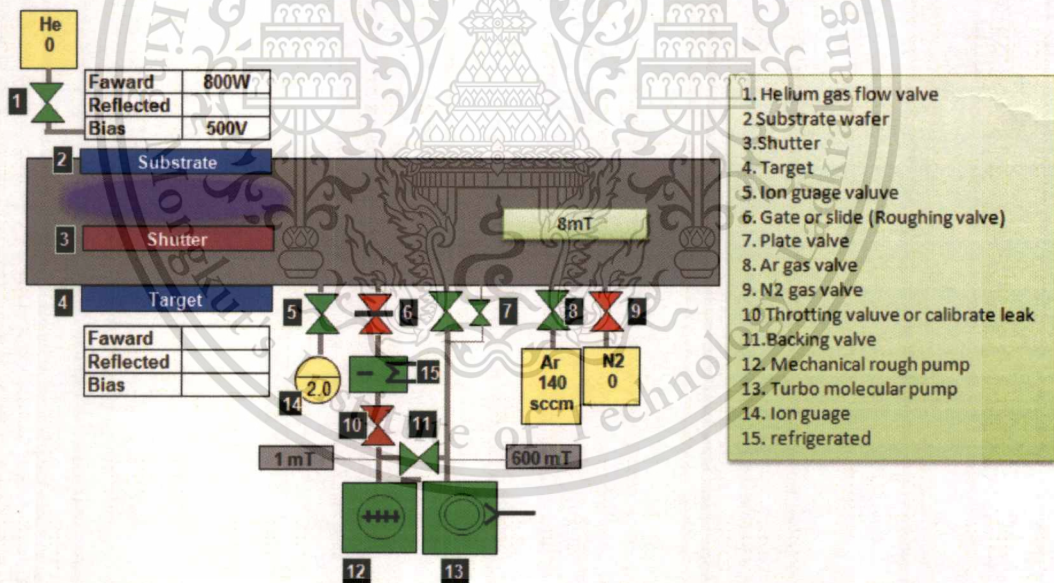


Figure 3.6: Vacuum pump system diagram of RF diode sputtering during pre-etch.

3.4.5 Pre-sputter step

Every time the chamber is opened for loading or unloading of substrates, the chamber and contents are exposed to atmosphere, resulting in the absorption of gases, including water vapor, by these elements. By pumping the system down to a high vacuum level most, but not all, of these absorbed gases will be removed, especially from the target. Alumina absorbs a large amount of water vapor when

exposed to atmosphere and to minimize sputtering contaminants affecting the substrates, a target cleaning step must be performed. This cleaning occurs prior to deposition on the substrates and is called pre-sputter (target pre-clean). A moveable shutter within the process chamber can be selectively placed between the target and the substrates. For pre-sputter, the shutter is inserted over the target. Target material is sputtered onto the bottom of the shutter instead of the substrates. This erodes the surface of the target, eliminating surface contaminants and water vapor. Material deposited on the bottom of the chamber must be periodically removed or the shutter replaced as a normal maintenance procedure. An additional benefit of pre-sputter is that the presence of active plasma tends to scrub the chamber walls, further reducing the level of contaminants.

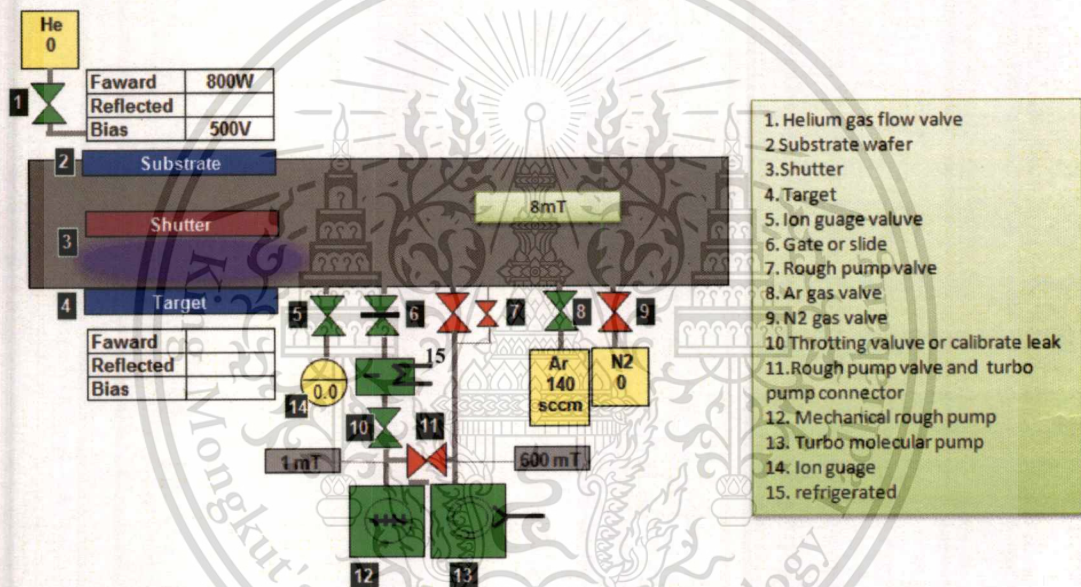


Figure 3.7: Vacuum pump system diagram of RF diode sputtering on pre-sputter step.

3.4.6 Deposition step

Deposit mode of operation consists of running a high level of RF (13.56 MHz) on the target, which results in sputtering material to the substrates above the target. During deposition the shutter is positioned out (not over target). Also, a low level of RF energy is applied to the substrate holder to generate a DC bias which helps dislodge any contaminant atoms which drift onto the substrate surface with the system operating in the deposit mode, the substrate RF power supply (1.5 kW) is run in a bias mode (the RF is self-adjusted to produce a fixed bias voltage). The applied power to the substrate is closed loop controlled to generate a specific bias voltage. If the measured bias voltage drops slightly, the RF generator increases the applied RF power to bring the bias back up to the desired level. In order to operate two

separate RF power supplies simultaneously, it is necessary to introduce a phase shift between the two. By running the two generators slightly out of phase, it is impossible for the two generators to either add or subtract to total power. For instance, if the two generators were 180 degrees out of phase, the peak-to-peak voltage of the lower power generator would be canceled. Also if both generators were precisely in phase, the total RF power would be additive.

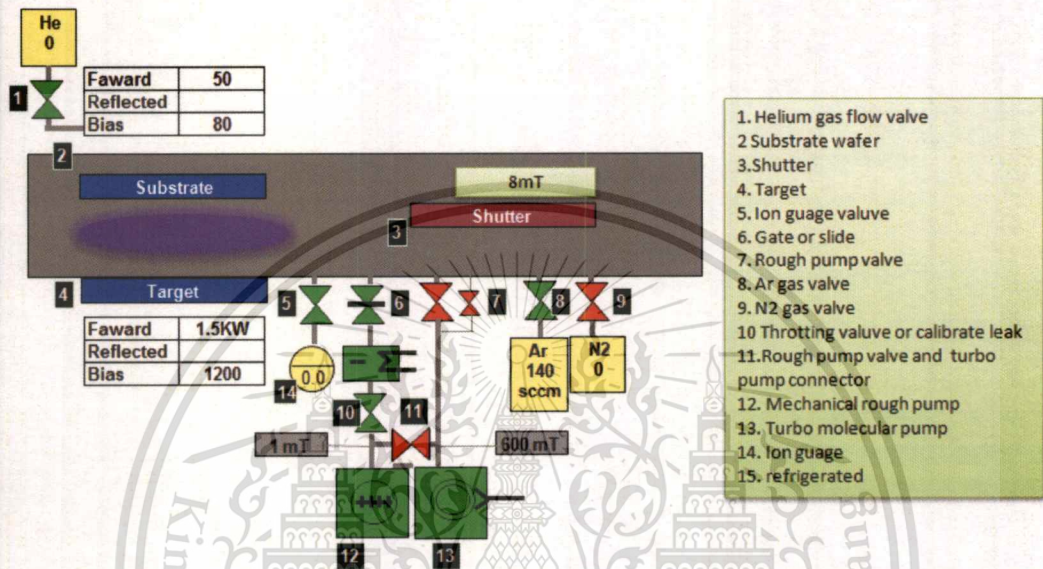


Figure 3.8: Vacuum pump system diagram of RF diode sputtering deposit step.

3.4.7 Vacuum gauge controller

The vacuum gauge controller measures pressure levels from the hot cathode ion gauge and transmits the data through the programmable logic controller to the computer control system. The vacuum gauge controller outputs an analog signal proportional to pressure. This signal is sent to the computer via an analog input module within the programmable logic controller. The computer also determines when to turn the ion gauge on and off. The ion gauge internal set points within the vacuum gauge controller are not used.

3.4.8 Thermocouple gauge

One thermocouple gauge is used to measure chamber pressure during the initial pump down stage. Thermocouple gauge gauges only measure from about 1 Torr to 10^{-4} Torr. A second thermocouple gauge (C on the vacuum gauge controller) is connected to the input of the mechanical pump (fore line). This thermocouple

gauge is useful for determining the condition of the mechanical pump and the fore line trap. As with the hot cathode ion gauge, the internal set points are not used.

3.4.9 MKS Baratron[®] Gauge

An additional vacuum sensing element is connected to the chamber for direct pressure measurement during deposition. This sensor is a capacitance manometer type device which measures pressure mechanically. This sensor differs from the previously discussed sensors in how it works and how it is used. The operating pressure range of this sensor is 0 to 1000 microns (1 Torr).

3.5 Characterization of chromium film

3.5.1 Film uniformity measurement by using micro head

The chromium coating was fabricated by RF sputtering on to ALTiC 6" wafers. The wafer was set Temp dot tape total 9 point on the wafer for thickness measuring by using micro head Tencorr as show Figure 3.9.

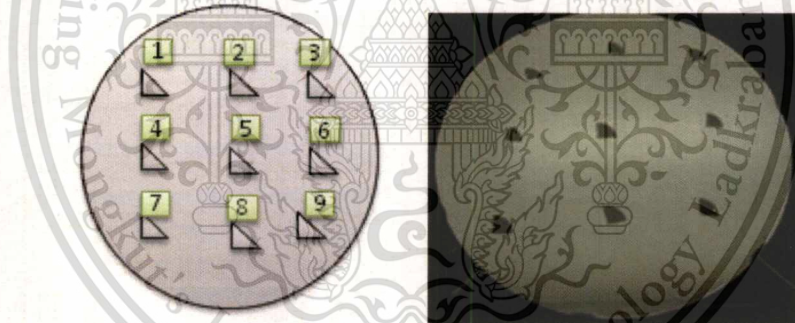


Figure 3.9: Thickness uniformity over 6" wafer substrate for provide sample.

There are nine point to do micro head measurement on wafers 6" for checking film uniformity six inch wafer was load to inside chamber of micro head Tencorr machine. After loading of the substrate distance was kept at 1 inch. Micro head check depth of chromium film automatically. In addition, we will consider each of these matrix for various each parameter. They are:

- Class A-A convex thickness profile. Thickness in the center of wafer and lower thickness at edges with uniformity less than 10 %
- Class B-A uniform with a concave profile (Higher deposit in edge of wafer)
- Class C-A uniform with a slope profile (one side deposit higher than another side)

This material is reserved for educational use only; not allowed for commercial use.

Forbidden to modify the content, and cite the document when use.

3.5.2 Surface hardness

The nano mechanical chromium film tests were investigated by nano-indenter (Triboscope, Hysitron, USA). The nano hardness and elastic modulus measurement, the nano indenter was set up with a North Star Cube corner diamond probe tip, 3-sided pyramidal indenter. The total included angle on this tip with 35.26 degrees, with a half angle of 17.63 degrees. The tip radius is less than 40 nm. The nano-indentation test under 50, 100, 200 until 300 μN loads

The holding time was 5 seconds for each incident. The nano hardness and elastic modulus of each incident was determined on the basis of Olivder and Pharr method [5]. The radius of curvature is less than 40 nm. ALTiC substrate were coated with chromium film by various substrate bias voltage -40V -80V -120V and -160V. All wafers were measured through nano-indenter for hardness and elastic modulus.

3.5.3 Thickness non-uniformity measurement

The area of wafer was 6 inch x 6 inch and comprised as nine points for thickness measurement by using micro head Tencorr machine. Step depth total 9 points were measured after coated chromium film. As a result, Wafer was measuring which have obtained from 9 points temp dot on the same wafer. Subsequently, we selected maximum and minimum values from 9 point applied equation to calculate the entire wafer uniformity.

3.6 Experiment varied substrate bias voltage

Chromium films were deposited by RF-Diode sputtering in Alcatel Comtech system. The system is having base pressure in a low 10^{-6} Torr region. We used high purity chromium target wt. % in purity 99.95%, which was sputtered with argon ions. The target-to-substrate distance was kept at 1.3 inch after loading of the substrate and target, the vacuum chamber was degassed down to 8 mTorr followed by inlet of argon gas. Before deposition, Cr was sputtered for 1 minute to clean the target surface. A thin Cr layer was deposited on ALTiC substrate during sputtering. The RF power for the target was fixed at 800W, the deposition time was 2 hours and the working temperature of the substrate was controlled by Helium pressure at 60°C . The thickness film is $2\ \mu\text{m}$. The base pressure of the chamber was less than 2×10^{-6} Torr. A negative bias was varied 40V, 80V, 120V and 160V. Deposition step was applied to all wafers sample under an Ar gas 140 sccm. And deposit pressure 8 mTorr. The deposition temperature was controlled at 25°C . Deposition time was fixed at 2 hours. The grain size structure was observed using SEM and the grain size distribution was measured using an image analyzer. For this propose, a slow scan

This material is reserved for educational use only, not allowed for commercial use.

image detector was used to explain the grain structure. The number for count grain was 200-400. The nano mechanical tests were investigated by means of nano-indenter (Triboscope, Hysitron, USA) interfaced with an atomic force microscopy (AFM , Nano scope XE-PTR) for the nano-hardness and elastic modulus measurement, the nano indenter was equipped with a Berkovich diamond probe tip. 3 sides pyramid indenter. The total included angle on this tip with 142.3 degrees with a half angle of 65.35 degree. The tip radius is around 100 nm. The nano indentation test was tested under 300 μN loads. The loading and unloading of the Nano hardness and elastic modulus of each indent was determined on the basis of Oliver and Pharr method [111] In order to eliminate the directional geometry difference, a conical shaped diamond probe was employed to conduct the nano wear test. The radius of curvature of the tip is less than 1 μm .

3.7 Conclusion

Chromium films have been deposited by RF diode sputtering technique with varied process parameters. The contamination involved in the process has been observed as the important criteria that influence the hardness roughness uniformity and contamination. Deposition rate was observed. The surface morphology shows a nature with comparatively surface roughness. From the investigations, It is clear that the energetic of process controlled by various factor included substrate bias voltage, deposit pressure and distance between two electrodes. Nano-indentation technique was investigated to identify which parameter of bias voltage given best hardness for using in wet etching process application. This studied to focusing on substrate bias voltage of chromium film on hardness and roughness includes grain size by SEM.

Chapter 4

Evaluations and results

In this study, the results and discussion would be presented into three parts. First part involved the effect of contamination by various plasma pressure parameter, substrate bias voltage and distance between electrodes on ALTiC surface of wafers. The second part was about the study of chromium film surface roughness. The last part involved the effect of plasma parameter on the mechanical properties and surface morphology of composites.

4.1 The effect of plasma pressure parameter on surface morphology of wafers

The problem in a preparation of wafer coating is dark spot on chromium film surface. Optimization of the pressure would be expected to enhance grain of chromium growth film and roughen the chromium surface. This would result in increasing bonding, physically between chromium film and the substrate. This part would concern the pressure parameter of growth film surface and its effects on morphology

4.1.1 Various substrate bias voltage

Various substrate bias voltages were investigated in order to find the optimum discharge power and substrate bias voltage of plasma reaction chamber for growth chromium film on the ALTiC substrate. KLA is observed contamination before/after coating film. The experiment result show in **Figure 4.1** for substrate biased voltage, varying from 40 V to 120 V with increment of 40 V was investigated. The results reveal the particle minimum at 40V

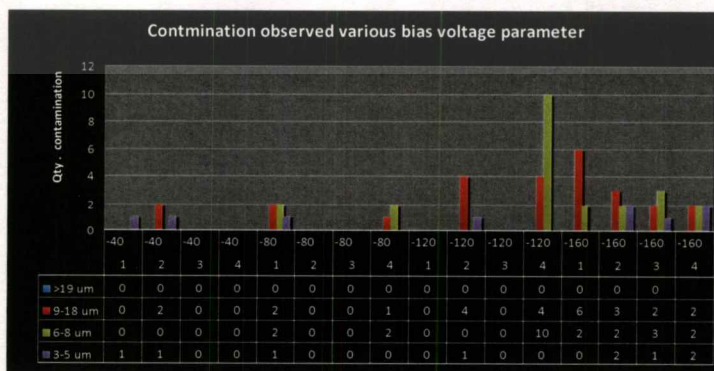


Figure 4.1: Surface defect with various substrate bias voltage parameter.

4.1.2 Various deposit pressure

Processing pressure varying 4, 8, 20 and 30 mTorr respectively was investigated. It found that the lowest level of contamination can be obtained at 4 mTorr. It shows contrast result with theory as we know that operating under low pressure as possible provides the most pure condition. This phenomenon is due to the particulate contaminations observed on film surface.

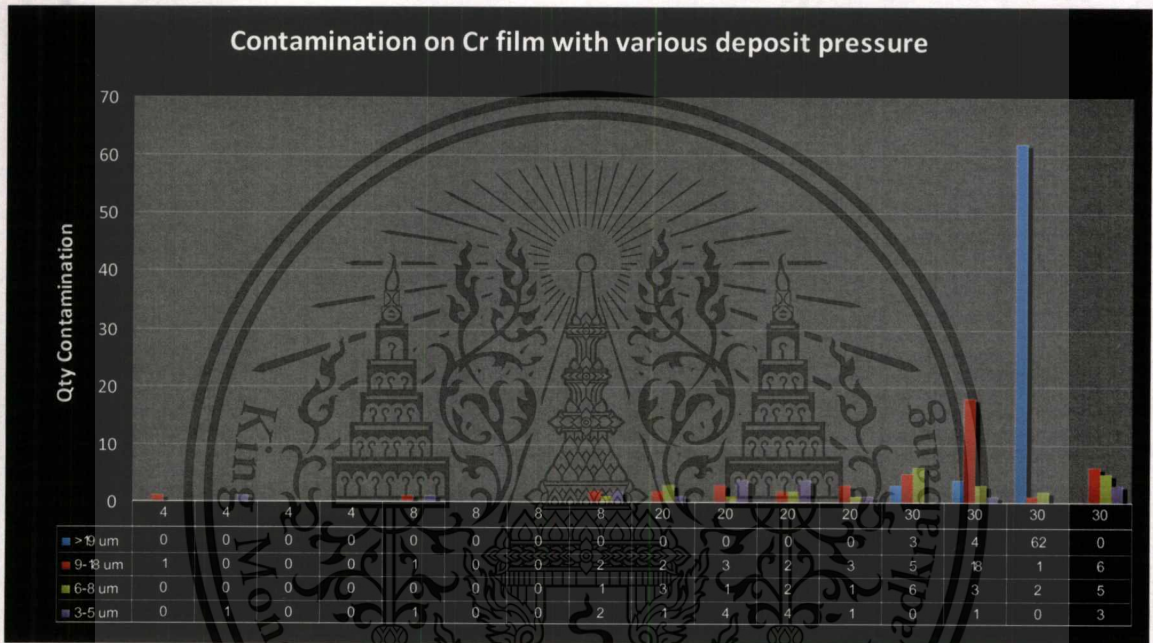


Figure 4.2: Surface defects with various deposit pressure parameter.

4.1.3 Various distance between electrodes

The distance between Substrate and target distance is various 1 inch 1.3 inch and 1.6 inch with RF power 1.5 kW. Particulate contaminations especially decrease at 1.6 inch when compared with 1 inch and 1.3 inch. Low substrate DC bias voltage make electric charge particle have low kinetic energy then the possibility of particle falling into or onto film surface is also lower than high DC bias voltage.

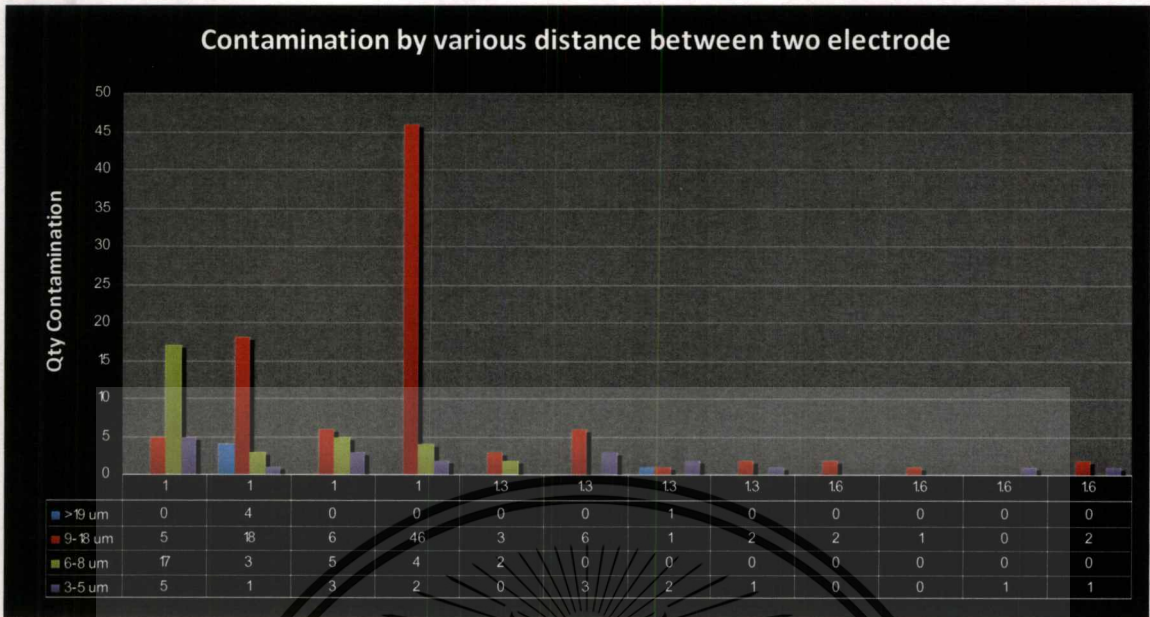


Figure 4.3: Surface defect with various distances between two electrodes.

The substrates coated with Chromium films were randomly selected to characterize and identify the contamination source. The particulate contaminations observed by KLA, cannot be observed by eyes view. Therefore, all of them were investigated through light power microscopy with 50X magnification and characterized by FE-SEM & EDX.

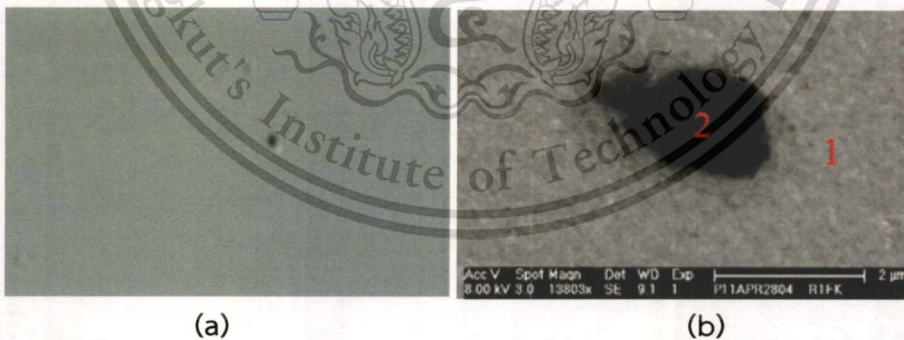


Figure 4.4: (a) Point defect is captured with high power microscopy and (b) SEM image show hole inside Cr film with approximately 5 μm diameter. The EDX detail at point 1 show composition of Cr, but at point 2 show composition of C substrate.



Figure 4.5: (a) Dark spot contamination is taken under high power microscopy. (b) SEM image show approximately 10 μm length. The EDX detail at point 1 show a composition of Cr film. But at point 2 show Cr and C.

Dark spot contamination may generate from chamber material or human who load/unload substrate to sputtering machine. Film deposition on the walls of the plasma chamber can flake due to thermal expansion mismatch, film stress, or from poor adhesion of the film to the wall.[4]

0.3 μm – 9.0 μm Cr particulates were observed on wafers. It may be created particulate contamination during two electrodes between the anode ground shield and the edge of the target. These particles appeared to be void or dark spot and exhibited random during plasma processing. After vent chamber and open the chamber, we found flake particle on the chromium target and beside target of chamber. With the plasma and current off and the particles in a motionless state, it caused the particle to temporarily due to the Coulomb force. Contamination results were recorded by KLA machine for surface contamination results with various parameter of sputtering parameter. For chromium sputtering, the nucleation processes are chosen minimum particulate contamination. Some dust is generated by the explosive of adsorbed water vapor during bombardment of the chromium target.

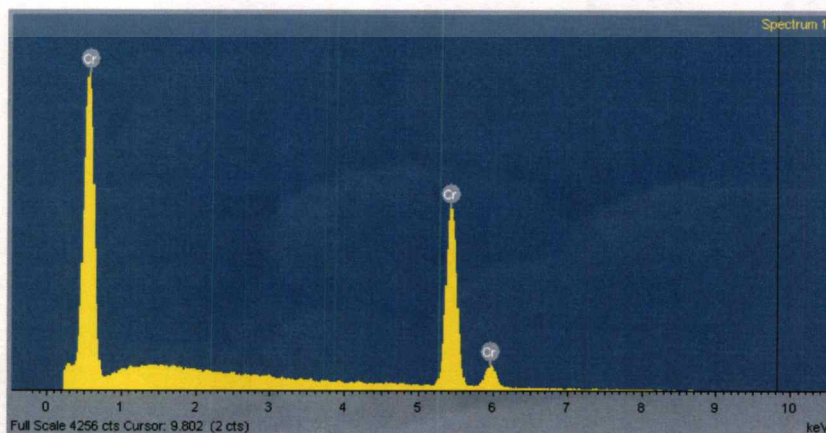


Figure 4.6: Particulate contamination results with EDX mode. owed for commercial use.

4.2 Study of film thickness non uniformity

4.2.1 Various substrate bias voltages

Film thickness is measured by using Tencorr micro head. Result of thickness represent chromium film coating rate per hour as show on **table 4.1**.

Table 4.1 Deposit rate various parameter

RF power	Pressure	Ar(sccm)	Bias(Volt)	Distance between electrodes (inch)	Average rate (um/hr)
1.5KW	Fixed @ 8mT	140	-40	Fixed @ 1.6 inch	1.16
1.5KW		140	-80		1.14
1.5KW		140	-120		1.02
1.5KW		140	-160		1.12
1.5KW	4mT	140	Fixed @ -80	Fixed @ 1.6 inch	1.10
1.5KW	8mT	140			1.13
1.5KW	20mT	140			1.15
1.5KW	30mT	140			1.15
1.5KW	Fixed @8 mT	140	Fixed @ -80	1	1.12
1.5KW		140		1.3	1.15
1.5KW		140		1.6	1.11

The results of the thickness uniformity measurements are shown in **Figure 4.7**. The uniformity was calculated as the maximum thickness minus the minimum thickness divided by twice the average to give the total range. The contours are in unit of $\mu\text{m}/\text{inch}^2$. The deposition of Chromium film thickness results gave a non-uniformity of +/- average 5.96% over an 6" substrate on wafer no.1.

4.2.2 Surface diagram with V_b -40V

The thickness non-uniformity of wafer no.1 is 7.82% wafer no.2 is 4.3% wafer no.3 is 6.8% and wafer no.4 4.93% overall thickness non uniformity is 5.96%.

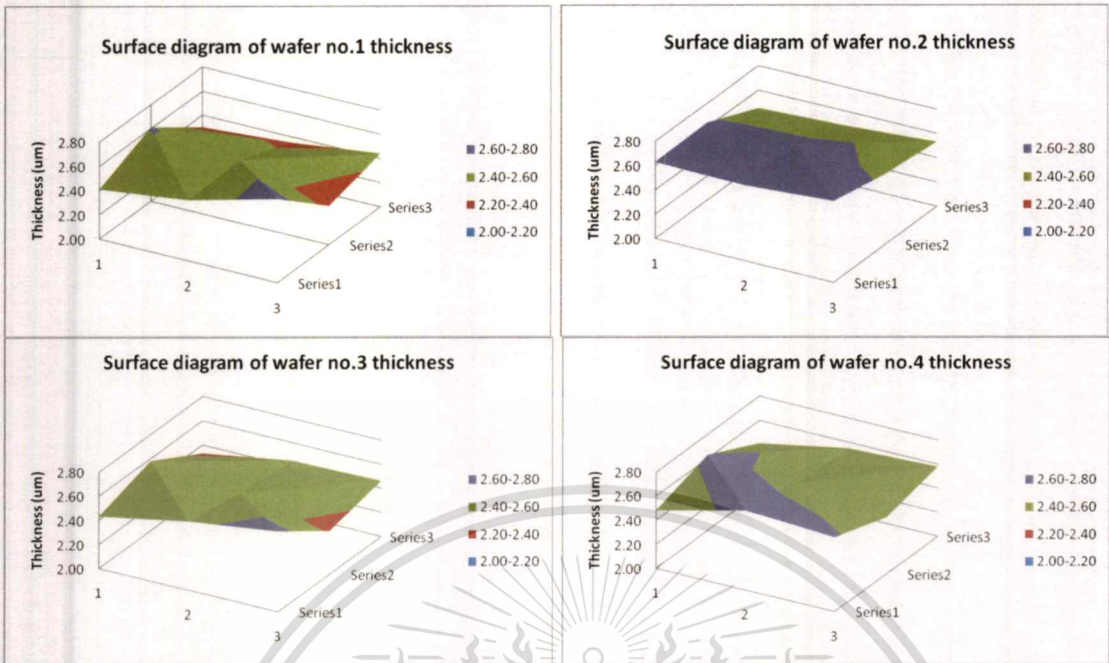


Figure 4.7: Surface diagram of chromium film with bias voltage -40V.

4.2.3 Surface diagram with V_b -80V

The thickness non uniformity of wafer no.1 is 9.44% wafer no.2 is 4.68% wafer no.3 is 8.93% and wafer no.4 6.83% overall thickness non uniformity is 7.47%

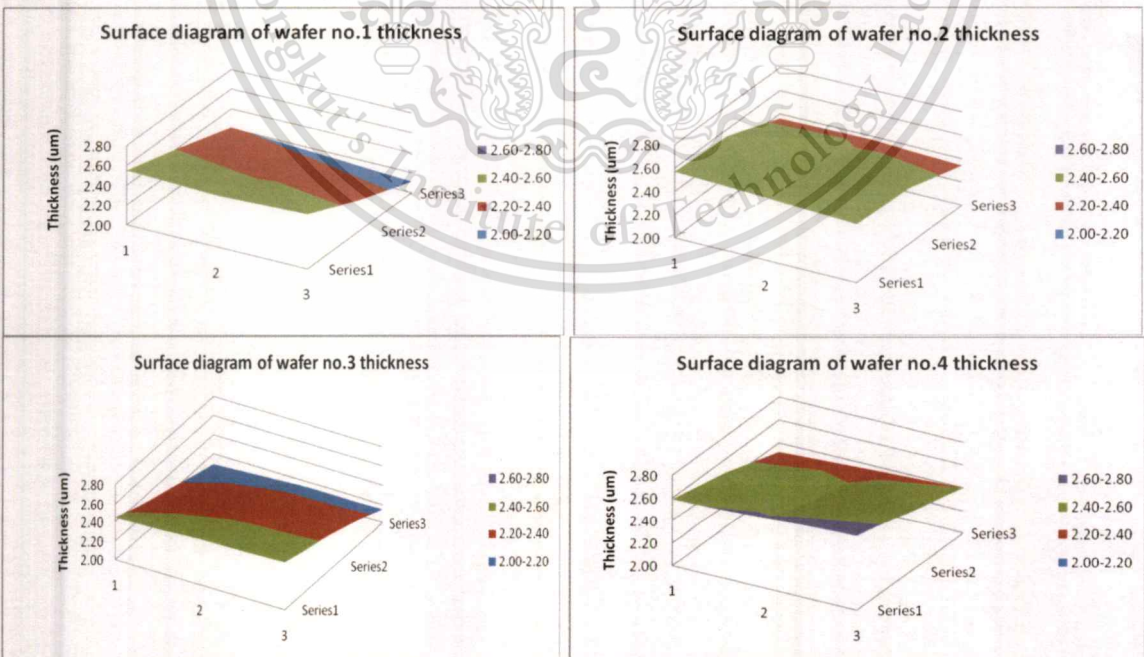


Figure 4.8: Surface diagram of chromium film with bias voltage -80V.

4.2.4 Surface diagram with V_b -120V

The thickness non uniformity of wafer no.1 is 8.70% wafer no.2 is 5.83% wafer no.3 is 5.63% and wafer no.4 7.36% overall thickness non uniformity is 6.75%.

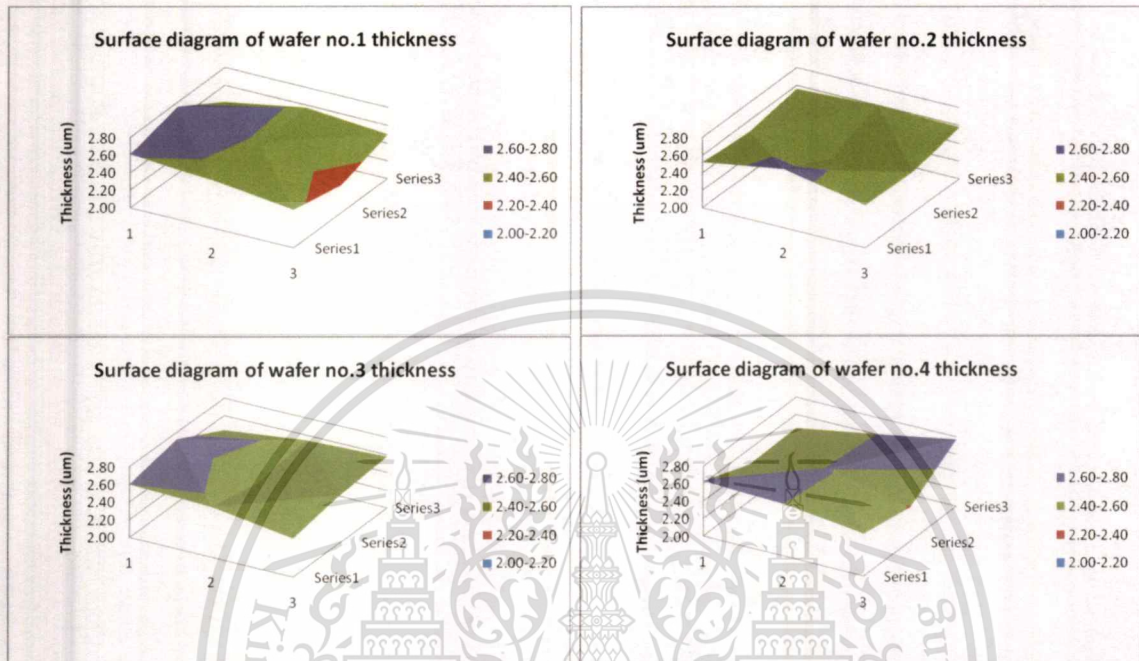


Figure 4.9: Surface diagram of chromium film with bias voltage -120V.

4.2.5 Surface diagram with V_b -160V

The thickness non uniformity of wafer no.1 is 7.63% wafer no.2 is 4.23% wafer no.3 is 5.93% and wafer no.4 7.03% overall thickness non uniformity is 6.20%.

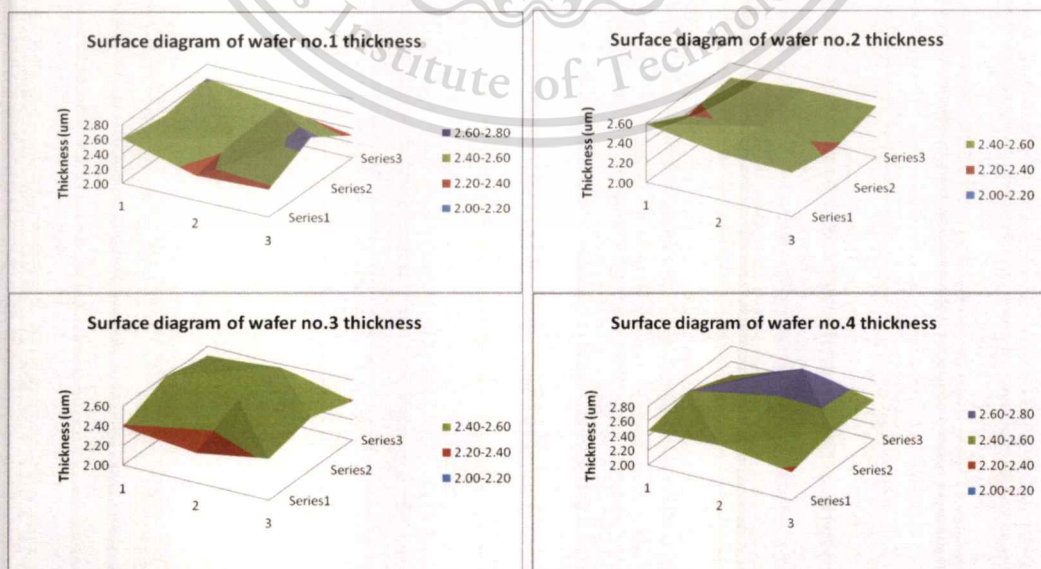


Figure 4.10: Surface diagram of chromium film with bias voltage -160V.

This material is reserved for educational use only, not allowed for commercial use.

Forbidden to modify the content, and cite the document when use.

Chromium film thickness were measured with various bias voltage by using micro head Tencorr step profiler. To compare bias voltage with increment -40V, Thickness non-uniformity has been characterized for a range of non-uniformities typical for negative bias voltage processing equipment as used in the semiconductor industry. Thickness non-uniformities is calculated and plot to surface diagram. It was found that thickness non-uniformities above the baseline 10%.

Table 4.1 compare uniformity vs various bias voltage and standard deviation of each parameter

Bias voltage	Average thickness (μm)	Max thickness (μm)	Min thickness (μm)	% non Uniformity
-40	2.52	2.67	2.37	5.96%
-80	2.40	2.57	2.22	7.47%
-120	2.54	2.73	2.38	6.75%
-160	2.48	2.65	2.34	6.20%

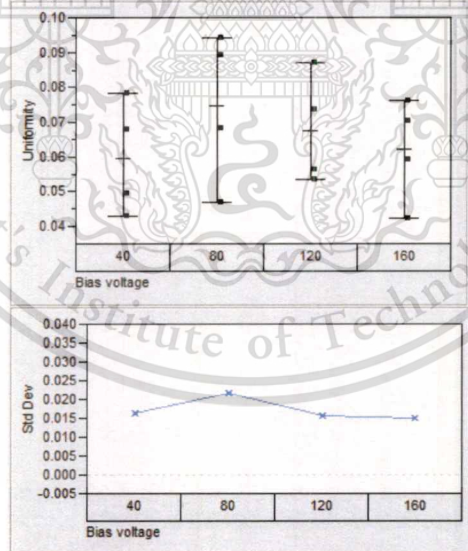


Figure 4.11: compare uniformity vs various bias voltage and standard deviation of each parameter.

All wafers thickness non-uniformity is comparable. Standard deviation each group no significant different. Experiment data was taken from profiler micro head measurement to obtain thickness profile. Bias voltage was various to observe non-uniformity profile. The data profile show no significant different with concave profile with non-uniformity 4-9%, standard deviation is 0.015-0.02, not allowed for commercial use.

4.2.6 Surface diagram with pressure 4 mT

The thickness non uniformity of wafer no.1 is 9.67% wafer no.2 is 4.31% wafer no.3 is 6.34% and wafer no.4 5.69% overall thickness non uniformity is 6.49%

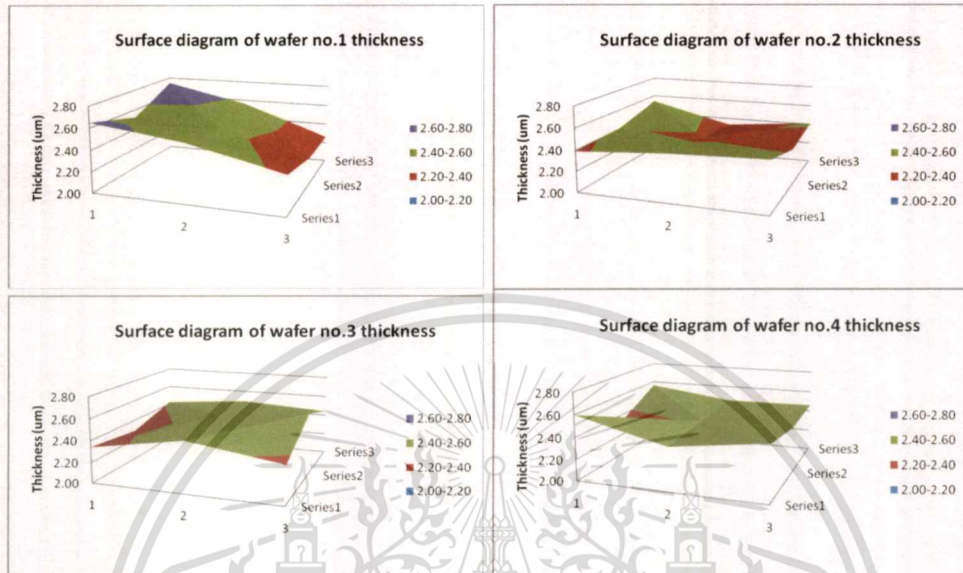


Figure 4.12: Surface diagram of chromium film with deposit pressure 4mT.

4.2.7 Surface diagram with pressure 8 mT

The thickness non uniformity of wafer no.1 is 9.44% wafer no.2 is 6.57% wafer no.3 is 8.84% and wafer no.4 4.07% overall thickness non uniformity is 7.23%

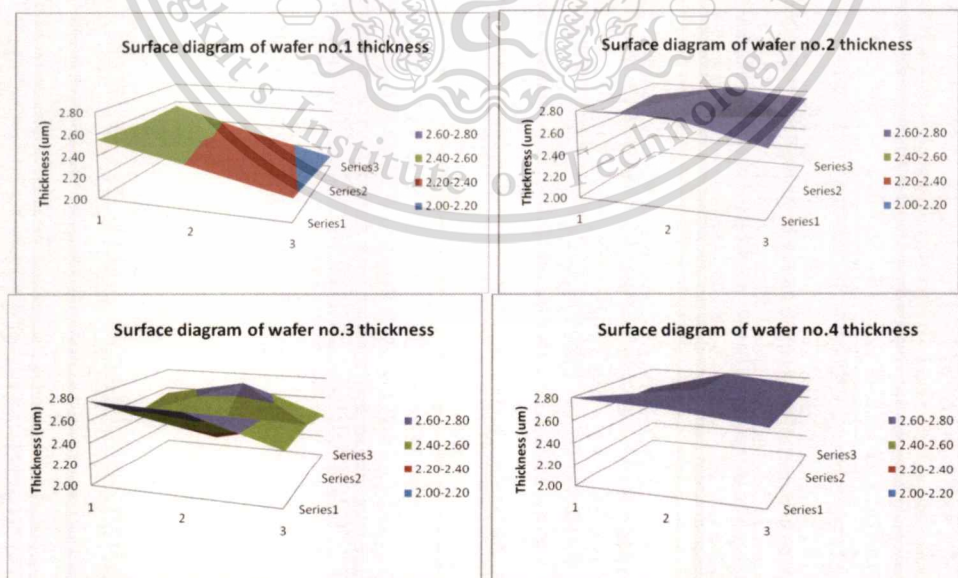


Figure 4.13: Surface diagram of chromium film with deposit pressure 8mT.

4.2.8 Surface diagram with pressure 20 mT

The thickness non uniformity of wafer no.1 is 6.10% wafer no.2 is 8.91% wafer no.3 is 8.05% and wafer no.4 4.25% overall thickness non uniformity is 6.94%

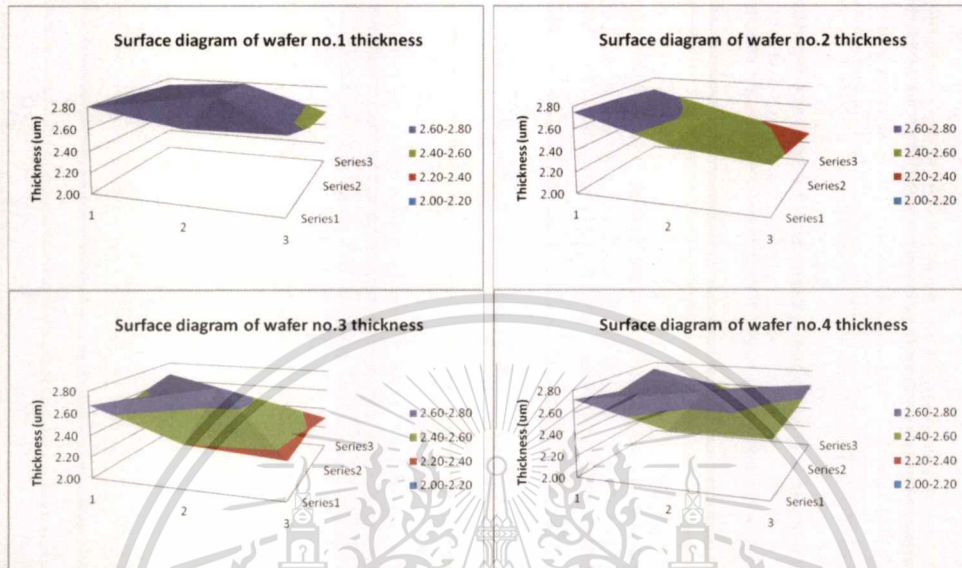


Figure 4.14: Surface diagram of chromium film with deposit pressure 20 mT.

4.2.9 Surface diagram with pressure 30 mT

The thickness non uniformity of wafer no.1 is 9.94% wafer no.2 is 5.4% wafer no.3 is 5.93% and wafer no.4 6.04% overall thickness non uniformity is 6.83%

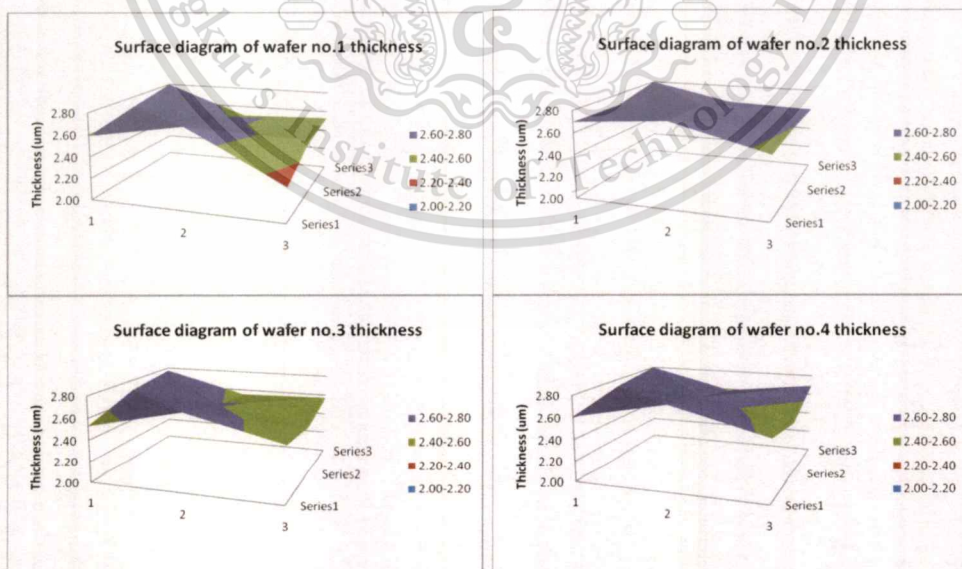


Figure 4.15: Surface diagram of chromium film with deposit pressure 30 mT.

Table 4.2 compare uniformity various deposit pressure parameter

Deposit pressure (mTorr)	Average thickness (μm)	Max thickness (μm)	Min thickness (μm)	%Non Uniformity
4	2.45	2.62	2.30	6.49%
8	2.59	2.76	2.40	7.23%
20	2.59	2.77	2.41	6.94%
30	2.64	2.81	2.46	6.83%

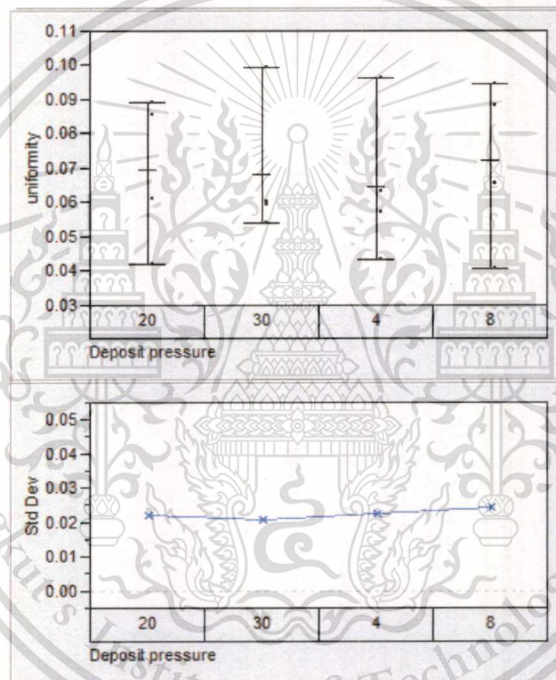


Figure 4.16: compare thickness uniformity vs various deposit pressure and standard deviation of each parameter.

All wafers thickness non-uniformity which have coated with various deposit pressure less than 10% specification. % Non-uniformity were comparable. Standard deviation each group no significant different with standard deviation 0.02.

4.2.10 Surface diagram with distance 1 inch

The thickness non uniformity of wafer no.1 is 5.58% wafer no.2 is 4.58% wafer no.3 is 6.59% and wafer no.4 6.11% overall thickness non uniformity is 5.71%.

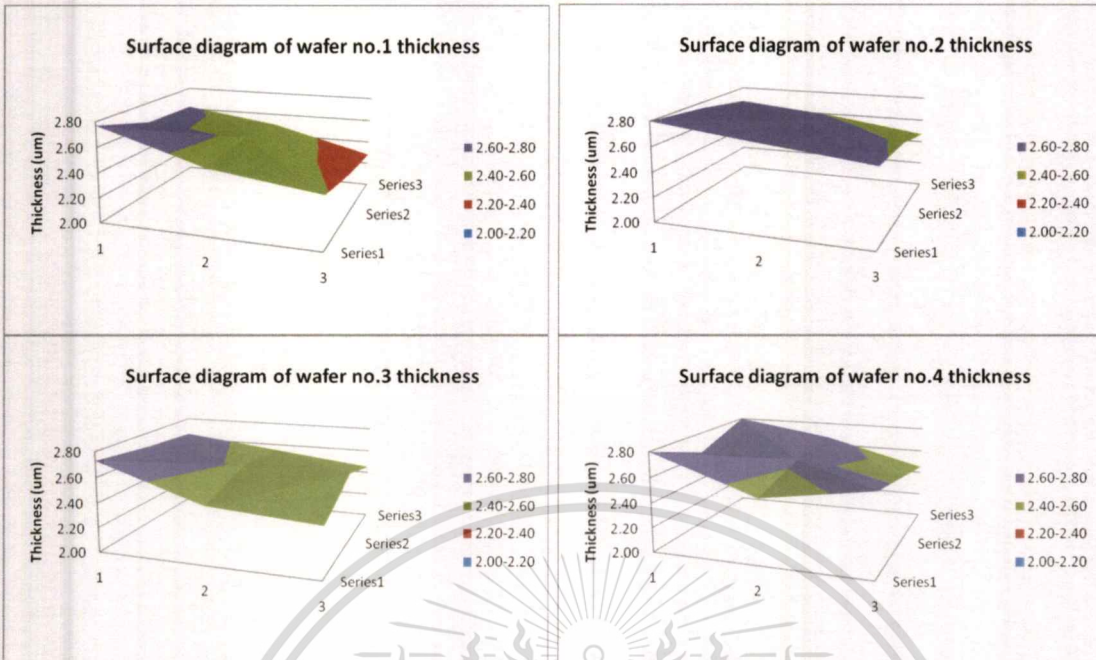


Figure 4.17: Surface diagram of chromium film with distance between 2 electrodes 1 inch.

4.4.11 Surface diagram with distance 1.3 inch

The thickness non uniformity of wafer no.1 is 6.10% wafer no.2 is 6.78% wafer no.3 is 8.55% and wafer no.4 6.55% overall thickness non uniformity is 7.00%

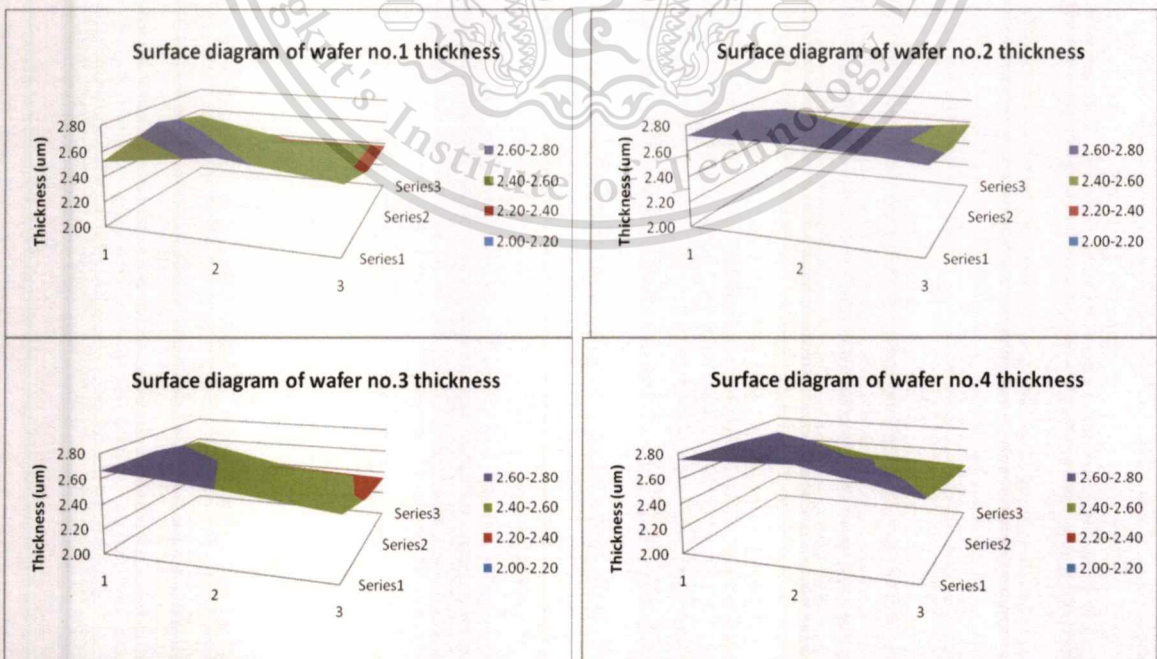


Figure 4.18: Surface diagram of chromium film with distance between 2 electrodes 1.3 inch.

This material is reserved for educational use only, not allowed for commercial use.

Forbidden to modify the content, and cite the document when use.

4.4.12 Surface diagram with distance 1.6 inch

The thickness non uniformity of wafer no.1 is 6.20% wafer no.2 is 4.84% wafer no.3 is 7.23% and wafer no.4 5.45% overall thickness non uniformity is 5.43%

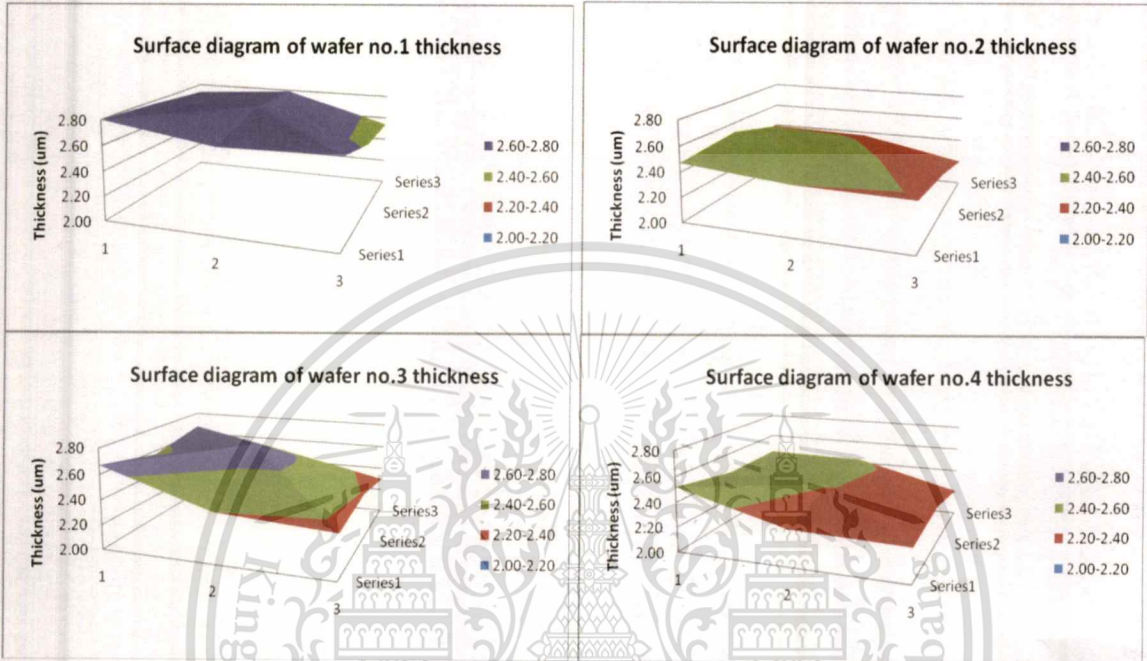


Figure 4.19: Surface diagram of chromium film with distance between 2 electrodes 1.6 inch.

Table 4.3 compares uniformity various distances between two electrodes

Distance between two electrodes (Inch)	Average thickness (μm)	Maximum thickness (μm)	Minimum thickness (μm)	%Non Uniformity
1.0	2.62	2.73	2.51	5.71%
1.3	2.64	2.74	2.50	7.00%
1.6	2.50	2.60	2.36	5.43%

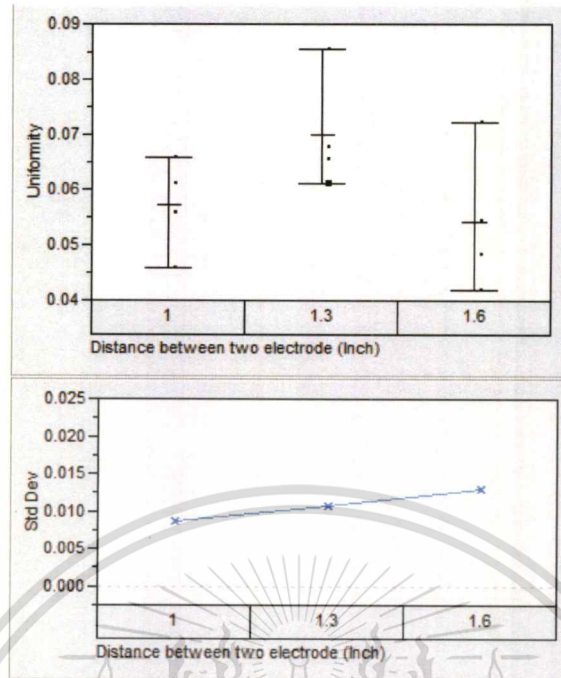


Figure 4.20: compare uniformity vs various distances between two electrodes and standard deviation of each parameter

All wafers thickness non-uniformity which have coated with various distance between two electrode less than 10% specification. % thickness non-uniformity were comparable. Standard deviation each group 0.01-0.015. The thickness non-uniformity of chromium film deposition were observed after film deposition. The highly non-uniform plasma density typical of RF diode sputtering processes are investigated.

4.3 Surface hardness

4.3.1 Hardness results by various negative bias voltage

Table 4.4 Hardness comparison by various substrate bias voltages

Force (μN)	Substrate bias voltage (Vb)	Average Hardness (GPa)	Contact depth (nm)
300	-40.0	5.21	193.15
300	-80.0	8.14	146.83
300	-120.0	7.79	152.35
300	-160.0	7.72	151.60

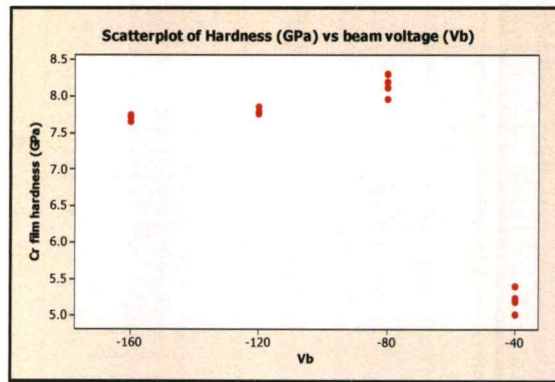


Figure 4.21: compare hardness results vs various bias voltage parameters

4.3.2 Hardness results by variuos deposit pressure

Table 4.5 Surface hardness of Cr film as function of deposit pressure

Force (μN)	Deposit pressure (mTorr)	Average Hardness (GPa)	Contact depth (nm)
300	4.0	7.32	49.00
300	8.0	9.66	38.48
300	12.0	9.52	42.51
300	16.0	9.05	45.43
300	20.0	9.12	40.41
300	30.0	9.78	38.07

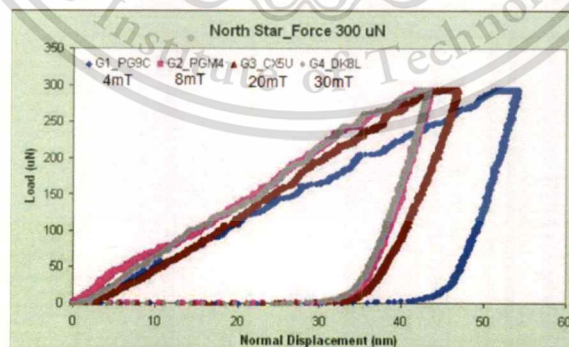


Figure 4.22: compare loading force and normal displacement by various deposit pressure

Surface hardness of two indent under 300 μN load on Cr coating analyzed by nano-indentation. Very sharp impressions can be observed. Loading forces versus penetration depths for the Cr film under 300 μN loads show good reproducibility of the

This material is reserved for educational use only, not allowed for commercial use.

Forbidden to modify the content, and cite the document when use.

test. The average nano-hardness data of chromium coating is 9 GPa with deposit pressure range 8-30 mTorr. Chromium films were measured with 300uN load for 6 different of deposition pressure group. Comparable hardness values of Chromium film manufactured in different methods are obtained by Lee et al and Oden et al [12,13]

The nano mechanical chromium film tests were investigated by nanoindenter (Triboscope, Hysitron, USA). The nano indenter was set up with a Berkovich diamond probe tip, 3-sided pyramidal indenter. The total included angle on this tip with 142.3 degrees, with a half angle of 65.35 degree

- Deposit pressure 8 mTorr, 12 mTorr, 16 mTorr, 20 mTorr and 30mTorr are high hardness
- 4 mTorr is the poorest hardness
- Based on hardness, Deposit pressure 4 mTorr is the poorest

4.4 Surface roughness and morphology of Cr film

The surface morphology of the Cr film analyzed by AFM is shown in Figure 1. Nodular grains ranging 80 nm in diameter are observed on the surface. Almost no surface defects such as macro particles and pinhole are found on surface. The average surface roughness (R_a) and Maximum peak-to-valley highest (R_{max}) are 6nm and 70 nm, respectively, as analyzed -40 Vb by AFM.

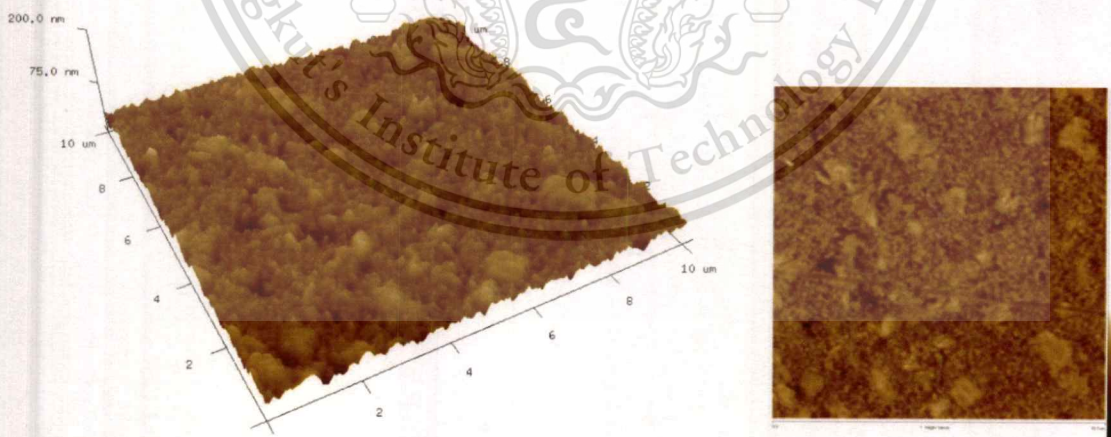


Figure 4.23: surface roughness of bias voltage -40 V.

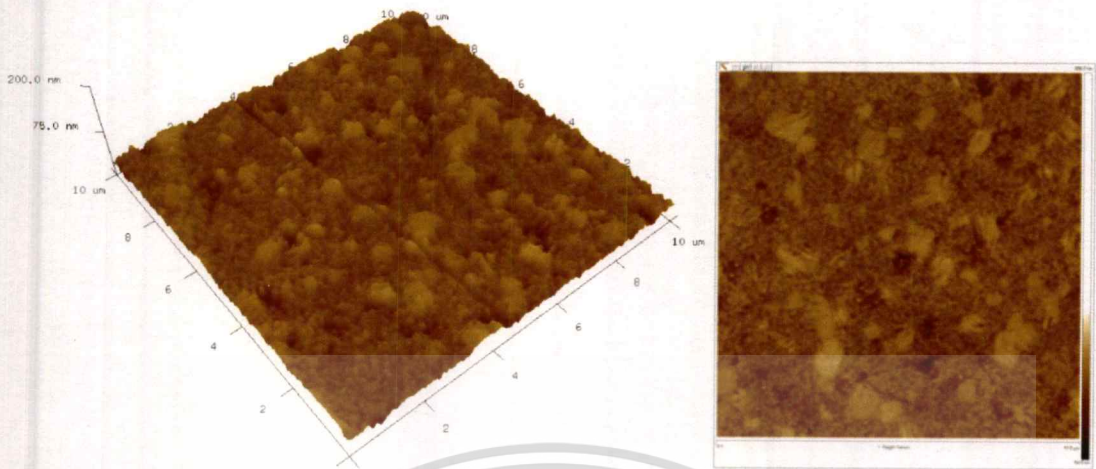


Figure 4.24: surface roughness of bias voltage -80 V.



Figure 4.25: surface roughness of bias voltage -120 V.

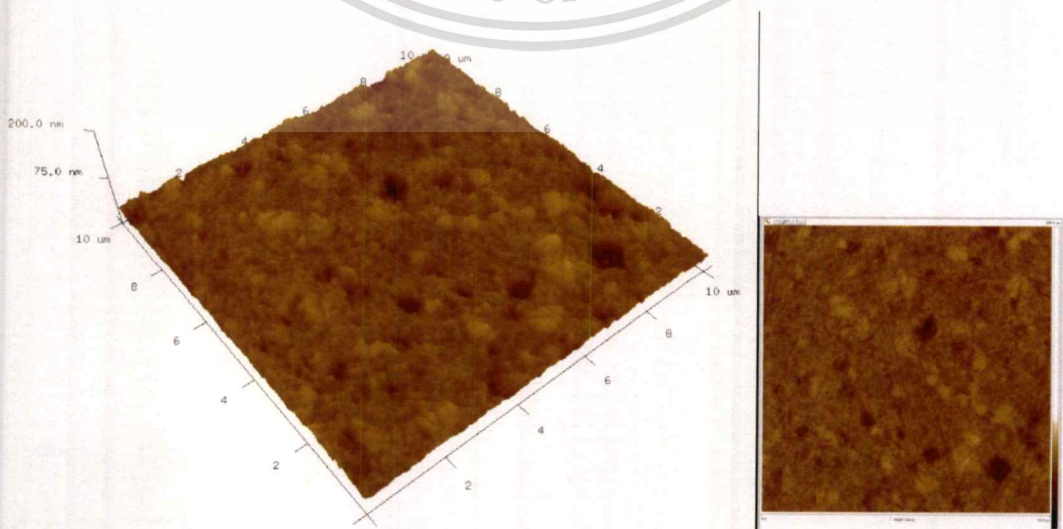


Figure 4.26: surface roughness of bias voltage -160 V. not allowed for commercial use.

The results from AFM studies (Figure 4.24-4.27). It was found that after coated with various beam voltage there were some particles and films on the Cr surface. From the AFM results, an arithmetic mean of the area roughness and area measurement were calculated as show table 4.3. The results showed that after various beam voltage parameters the average roughness (R_a), root-mean-square roughness (R_{Rms}), and surface area were increased. The results from AFM study confirmed the beam voltage parameter caused the decrease in the surface roughness of chromium film.

Table 4.6 arithmetic mean of the area roughness average roughness, R root mean square and R_{max} .

Wafer roughness (nm)			
Beam voltage	Ra	Rms	Rmax
-40	5.830	7.500	70.900
-40	5.740	7.320	66.600
-40	5.740	7.350	64.500
-80	5.420	7.030	57.900
-80	5.210	6.760	54.000
-80	5.180	6.670	52.500
-120	4.440	5.710	46.700
-120	4.430	5.660	48.900
-120	4.390	5.720	46.000
-160	4.250	5.660	59.300
-160	3.910	5.130	54.900
-160	3.760	5.040	54.200

In physical vapor deposition (PVD) processes, the coating is deposited in vacuum by condensation from a flux of neutral or ionized atoms of chromium metals. In the case of various bias voltage of the target sputtering, atoms are ejected mechanically from a target by the impact of ions or energetic neutral atoms. -160V given average roughness smooth coating surface with roughness 3.7-4.2 nm, Roughness especially increase when increasing target bias voltage. The film roughness for chromium deposited on AlTiC wafer substrates has been investigated for different substrate bias voltages. The AlTiC substrates were first mechanically polished to meet roughness target approximately 2 nm. Figure 4.27 show the coating roughness graph (R_a) results when V_s varies. It is evident that the increase in substrate bias voltage (V_s) leads to decrease roughness. These studied related to more efficient ionic bombardment of glowing film when V_s increase, a better arrangement of the glowing layer should be come from higher mobility of the ad-atoms. The growth of chromium ions condensed on the substrate surface are therefore able to move more easily given decreasing roughness results.

This material is reserved for educational use only, not allowed for commercial use.

Forbidden to modify the content, and cite the document when use.

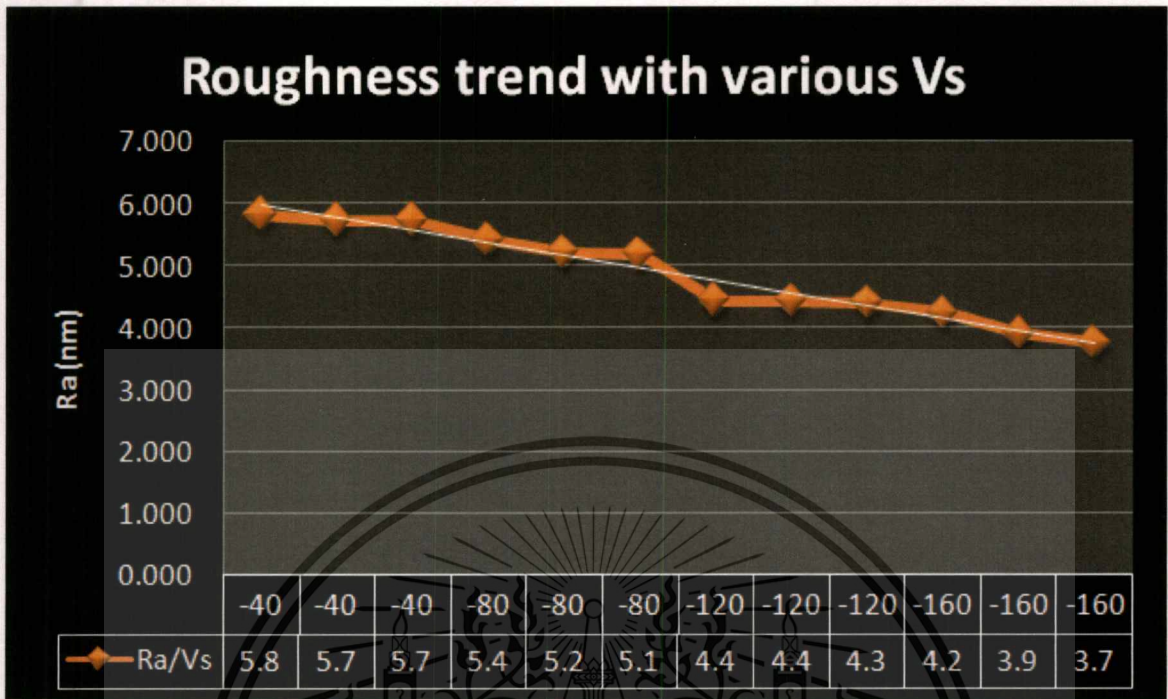


Figure 4.27: the roughness of chromium film deposit on ALTiC substrate at different bias voltage.

4.5 SEM micrograph surface grain the fractured surfaces of Cr

SEM technique was used to characterize the surface of chromium film after coated with substrate bias -160V. Cr grain size was observed at 20,000X and 50,000 X magnifications. The deposited grain structure of Cr thin films varied substrate bias voltage. The micrographs indicate that a significant grain growth occurs during RF diode sputtering at increasing substrate bias voltage. One of the possible reasons for this is that a strong negative bias applied to the depositing film has the effect of significantly enhancing the ad-atom mobility through the bombardment action of a positively charged Ar^+ ion. Figure 4.28 shows the variation of average grain size with Cr content of substrate bias with negative 160V films. It is obvious that average grain size of the film is increasing as bias voltage. Average grain size is about 50 nm at bias voltage 160V. but it increased to about 200 nm as bias voltage 40V. The EDS analyses indicate that the composition of grain consists of Cr material purely. These results reveal that most of Cr exists in the grain boundary and it restrains the grain growth during deposit, therefore, proposed that the grain become smaller with increasing bias voltage. This has resulted decreased inter grain size to support hardmask coating for etch selectivity with high resistance.



Figure 4.28: Grain of chromium film with substrate bias -160V, SEM image 20,000 X and 50,000X magnification.

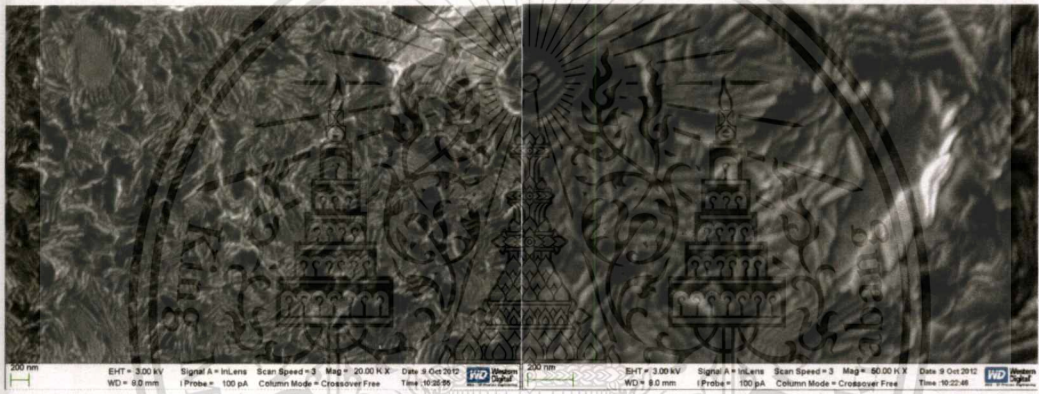


Figure 4.29: Grain of chromium film with substrate bias -120V, SEM image 20,000 X and 50,000X magnification.

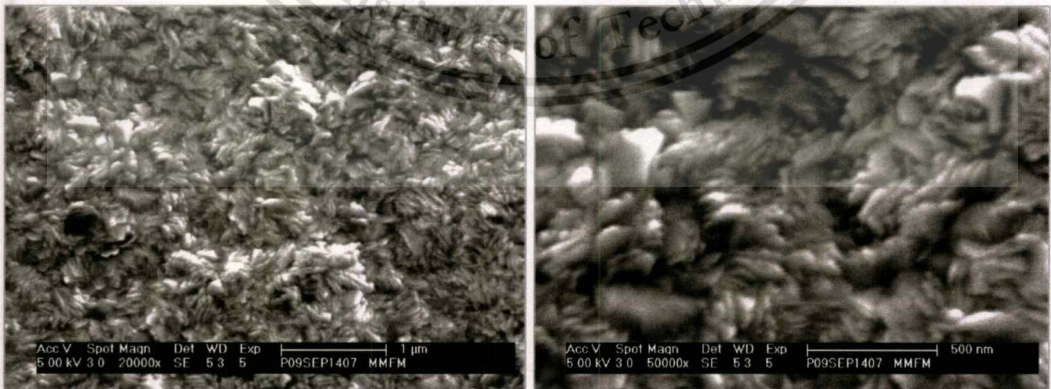


Figure 4.30: Grain of chromium film with substrate bias -80V, SEM image 20,000 X and 50,000X magnification.

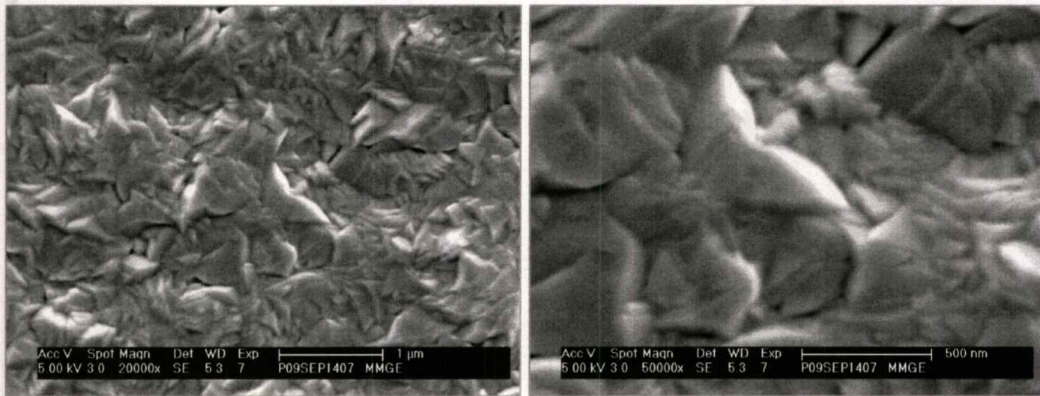


Figure 4.31: Grain of chromium film with substrate bias -40V, SEM image 20,000 X and 50,000X magnification.

From **Figures 4.28 – 4.31**, it can be seen that fractured surfaces of chromium film by various deposit bias voltage show that -40V given biggest grain size and highest roughness. Clearer pictures can be seen in Figure on the right hand side at 50,000 X magnification. Substrate surface displayed an irregular film formation with ALTiC substrate increase with substrate bias voltage. From SEM micrographs, the semiquantitative measurements of the Chromium film grain size ranged from 90-200 nm, the results related to surface roughness -160V given extreme roughness with smallest grain size. The mechanism of the grain formation is mainly due to internal stress in the coating, if the energy enough to forming small grain of growth film. However, in this case the grain size and roughness related also show an important quantity of chromium, which is indicative of film hardness quality. Substrate bias voltage parameter show interesting differences grain size to ALTiC wafer substrate. In this case, high magnification (500 nm) can be distinguished. Specially, The Chromium surface of -40V consist of big crystal randomly distributed on the surface and whole size was larger than obtained on the various substrate bias voltage at -80 -120 and -160 V. These result also suggested that small grain size, low roughness given better hardness on ALTiC substrate. In addition, it is necessary to consider that may be occur surface defects on substrate during coating growth, which can cause locally defects or dark spot areas.

The contamination results is seen that plasma parameter cause of contamination during sputtering process. The results create by KLA laser particle measurement on the wafer substrate. Eventually this results in fracture of deposit pressure distance between two electrode of contaminant into plasma. Once there. The particle is rapidly becomes heated and electrons neutralization by ion bombardment. The results in deposit parameter on surface showing void defect. The particle during deposition may move fast and can become sufficiently hot to become embedded into substrate. The mechanism summarized above will describe in detail below.

This material is reserved for educational use only, not allowed for commercial use.

Forbidden to modify the content, and cite the document when use.

- a) For chromium sputtering , The nucleation process is likely initiated by Argon gas bombard the chromium target which have generated upon initiation of the plasma, become charged and then trapping effects near the surface of the target. Particle can be generated during chamber maintenance.
- b) It also possible that the deposit pressure contributes kinetic energy to the momentum of particle from inside of chamber. Changing size of particulate result on substrate caused distance between two electrode glow discharge are often contaminated by particulates resulting from gas phase nucleation or sputtering of surfaces in contact with the plasma. If these particulate are sufficiently large, They will negatively charge and act as coulomb-like scattering centers for electrons. In doing so , rate coefficients for high-threshold process such as ionization may be reduced compare to those in pristine plasmas. If the contamination is non uniform, then the resulting spatial irregularities in the rates of excitation may lead to plasma properties which are also nonuniform. In this studied, we studied on the results of contamination for argon glow discharges contaminated by dust.
- c) The wafer uniformities of chromium film reached less than 10% with studied of various parameter of pressure negative substrate bias voltage and distance between two electrode. All uniformity results show pass specification. And all parameter given convex shape of uniformity. The optimum condition parameter is -80V substrate bias voltage 8 mT deposit pressure and 1.6 inch distance between two electrode. This result save more time and rework maintaining the sputtering solution improving surface defects and contamination control support PVD process.

CHAPTER 5

Conclusion and Suggestion

5.1 Conclusion

Part I: The effect of surface contamination on Chromium surface with various coating parameter

In this study, the effect of contamination deposit parameter consist of 3 parts. Firstly, various bias voltage, secondly, deposit pressure and thirdly, distance between two electrodes on RF diode sputtering system was investigated.

Attempts had been made to improve the contamination on wafers by various deposit parameters. The following conclusions could be drawn:

1. Surface of chromium film by various distances between two electrodes, Deposit chromium hard mask film on ALTiC. Optimum distance at 1.6 inch could be improving particulate contamination on chromium film significantly.
2. Surface of chromium film by various deposit pressure, 4mT to improvement of contamination on size 3-10 μm significant
3. The fractured surface of the composites with increasing bias voltage higher proportion of contamination on chromium surface from the metric. This might be due to the mechanical improving of the physical force from the surface roughness.

Part II: The non-uniformity of chromium surface with various coating parameter

Normally wafer were coated chromium film using hard mask for etch selectivity with high etch depth 1-10 μm range. Uniformities of chromium film are main factor for calculate depth of patterning etch selectivity on wet etching process. PVD RF sputtering plasma parameters were studied, uniformity on 6 inches wafers with micro-head. The uniformity results show pass specification with less than 10%. And no significant change of uniformity is observed, as the loading of deposit pressure bias voltage or distance between two electrodes were increased.

Part 3: Study of hardness of chromium film with various deposit parameters

This study, we found that chromium film have hardness with range 5-9 GPa with thickness approximate 2 μm . Minimum hardness result with low bias voltage 40V, especially increase to 9 GPa after adjust bias voltage parameter over 80V, 120V, 160V respectively. The nano-indentation results given more than 8 GPa hardness

which have using in the process. The hardness could be significant improve when increasing deposit pressure to 8 mTorr.

Part 4 Study of roughness of chromium film with various negative bias parameter

The results given average roughness decreasing with increasing higher negative bias voltage -160V average roughness is 3.7-4.2 nm. The grain size of -160V is small to getting highest grain.

From the experimental results, the optimum conditions for obtaining the lowest level of particulate contamination is 8 mTorr, 40 V and 1.6 inch for process pressure, substrate bias voltage and gap distance between the substrate and target. According to EDX results, the contamination on film surface may come from various sources, such as from target, substrate, and sputtering system component. After that surface roughness, surface thickness non-uniformity, surface morphology, surface hardness and Nano-indentation were observed in various process parameters, the optimum conditions result from parameter negative bias voltage 160V 8 mTorr deposit pressure and 1.6 inch distance between two electrodes given the good roughness with R_a 3.7 nm 9.5 GPa hardness and excellent surface hardness which have given increasing grain structure.

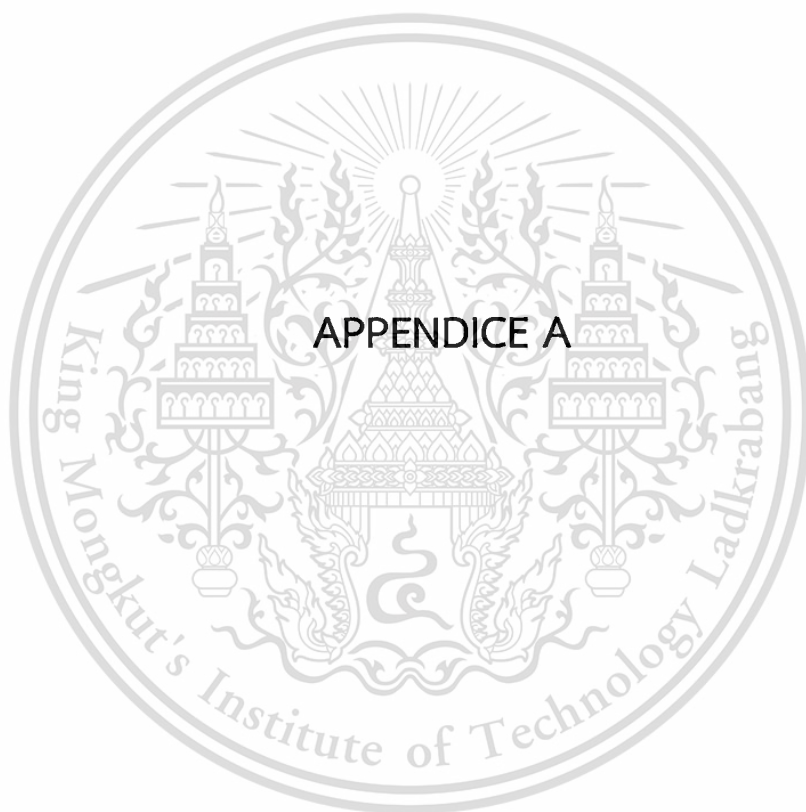
5.2 Suggestion for further work

1. Chromium film is deposited on AlTiC substrate by using RF diode sputtering. Energy during deposition has influence to structure of film. The effect of conditions in plasma deposition should be investigated in more details such as flow rate, deposition time and phase diagram of chromium.
2. To analyze more mechanical properties of chromium film such as tribology scratch test.
3. To analyze cross section by using TEM for study film of nano structure.
4. To do evaluation on other material or do reactive gas such as nitrogen.

REFERENCES

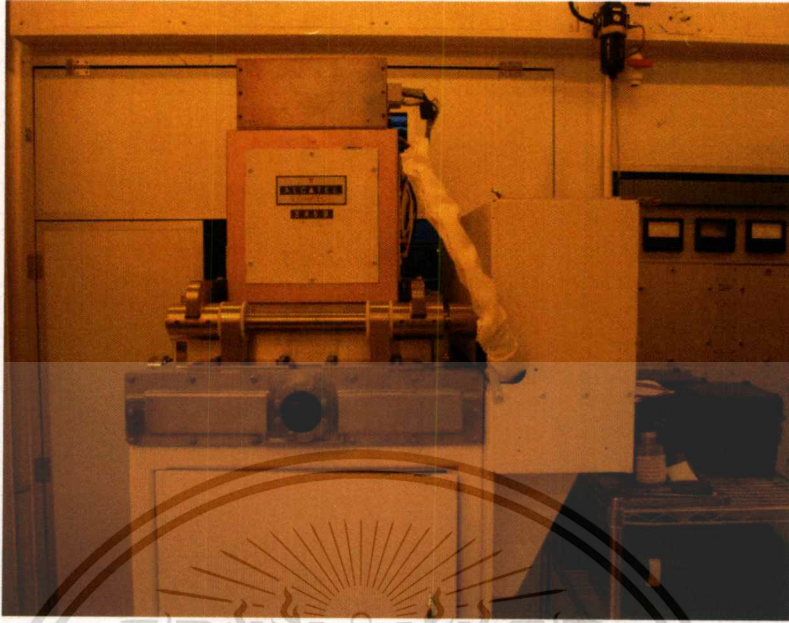
- [1] Z. Ahmed, T. Donnelly, P. J. Davey, and W. W. Clegg, "Increased areal density using a 2-dimensional approach," *IEEE Transactions on Magnetics*, vol. 37, no. 4, pp. 1896–1898, 2001.
- [2] I. Milošev, H. Strehblow, B. Navinšek, *Thin Solid Films* 303 246. 1997.
- [3] A. Conde, G. Fuentes, T. Tate "Surface & Coatings Technology" pp. 3588–3595, 2006.
- [4] W. J. Bertram, *VLSI Technology* McGraw-Hill. pp. 600-605 1983.
- [5] J. F. O'Hanlon and H. Parks. *J. Vac. Sci. Technol. A*. 10. pp.1863, 1992.
- [6] G. S. Seiwyn, "particle contamination formation and detection in magnetron sputtering processed", International thin film conference.
- [7] G. S. Seiwyn, "Particles and Gases and Liquids 3: Detection. Characterization and Control", (ed. K. L. Mittal), Plenum Press, pp 213-222 1993.
- [8] M. Baker, P. Kencha, M. Joseph, C. Tsotsos, A. Leyland, A. Matthews, *Surf. Coat. Technol.* 162 (2004) 222.
- [9] D.P. Ravipati, W.G. Haines and J.L. Dockendorf, J. "Vacuum Science Technology", A5.(4) 1987.
- [10] Ji, A.L., and Et al., "Micro structures and mechanical properties of chromium oxide films by arc ion plating", *Materials letters*, Vol. 58, pp.1993-1998 2004.
- [11] Butilenko, V., A.K., Vovk, A.Y., and Khan, H.R., "Structure and electrical properties of cathodic sputtered thin chromium films", *Surface & Coating Technology*, Vol.107, pp.197-199. 1998.
- [12] Moise, V., Cloots, R., and Rulmont, A., "Study of the electrochemical synthesis of selective black coating absorbing solar energy", *International Journal of Inorganic Materials*, Vol.3, pp1323-1329. 2001.
- [13] Duchemin D., "An Investigation of Ion Engine Erosion by Low Energy Sputtering", *Ph.D. Dissertation*, California Institute of Technology, Pasadena, CA, 2001.
- [14] Feldman L., Mayer J., "Fundamentals of Surface and Thin Film Analysis", North Holland-Elsevier, Prentice Hall, New York (1986)
- [15] Smith, D.L., 1995, *Thin Film Deposition :Principle and Practice*, New York, McGraw-Hill, pp.616
- [16] Bunsha, R.F, *Handbook of Deposition Technologies for thin Film and coating*, 2nd ed., New Jersey, Noyes Publication, pp.861, 1994.

- [17] Rohde, S.L. and Munz, W.D., "Sputtering Deposition" in *Advance Surface Coating: A Handbook of Surface Engineering*, New York, Chapman and Hall, pp. 103-105. 1991.
- [18] Munz, W.D., 1991, "The Unbalanced Magnetron: Current Status of Development", *Surf. Coat Technology*, Vol 48, pp. 81-94
- [19] Anguelouch, A., and Et al., "Properties of epitaxial chromium oxide films grown by chemical vapor deposition using a liquid precursor", *Journal of Applied Physics*, Vol.91, No.10, pp.7140-7142. 2002.
- [20] Teixeira, V., and Et al., 2002, "Chromium-base thin sputtered composite coatings for solar thermal collector", *Surface Engineer, Surface Instrumentation & Coatings Technology*, Vol.107, pp.197-199
- [21] Hones, P., Diserens, M., and LEVY, F., "Characterization of sputter-deposited Chromium oxide thin films", *Surface & Coatings Technology*, Vol. 120-121, pp.277-283, 1999.
- [22] D.J. Stirland, "Electron Bombardment Incuced Changes in the Growth and Epitaxy of Evaporated Gold Films," *Appl Phyhs Lett.*, Vol. 8, No.12, pp.326-328, 1966.
- [23] J.A.Venable, "Kinetic Studies of Nucleation and Growth at Surfaces," *Thin solid film.*, Vol.50, pp. 357-359, 1978.
- [24] R.M. Hill, "Electrical Conduction in Discontinuous Metal Films," *Contemp.Phys.*, Vol. 10, No.3, pp.221-240, 1969.
- [25] K.H. Behrndt, "Influence of the Deposition Conditions on Growth and Structure of Evaporated Films," *Vacuum*, Vol 13, pp.337-347, 1963.
- [26] Wasa, K and Hayakawa, Sl, *Handbook of Sputter Depositon Technology :Principles, Technology and Applications*, New Jersey, Noyes Publications, pp.19-29 1992
- [27] Maissel, L.I. and Gland, R., *Handbook of Thin Film Technology*, New York, McGrawhill, pp. 1-23 1970.
- [28] Vossen, J.L. and Kerns, W., *Thin Film Process*, New York, Academic Press, pp. 552 1978.
- [29] Smith, D.L , *Thin Film Deposition :Principle and Practice*, New York, McGraw-Hill, pp.616 1995.
- [30] Bunshah, R.F., *Handbook of Deposition Technologies for Film and Coating*, 2nd ed., New Jersey, Noyes Pulblication, pp. 861 1994.

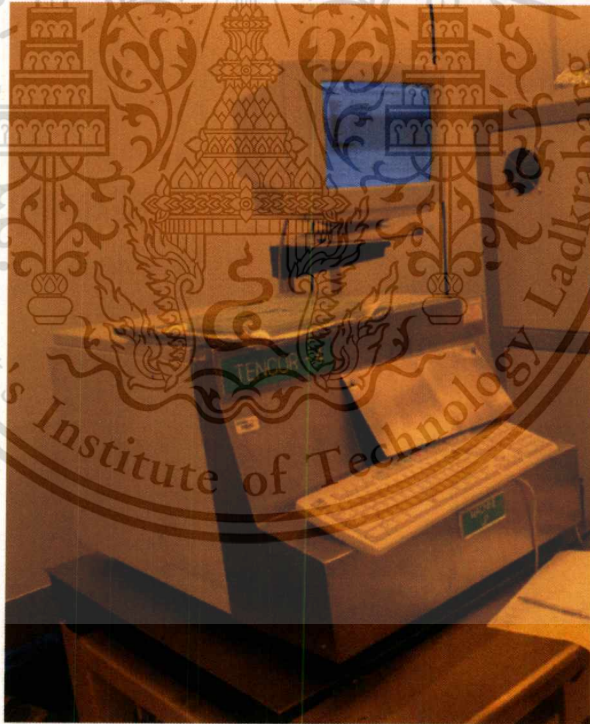


This material is reserved for educational use only, not allowed for commercial use.

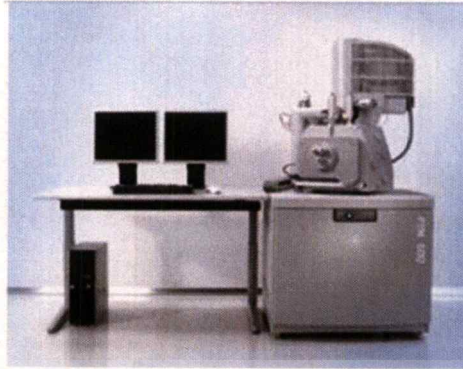
Forbidden to modify the content, and cite the document when use.



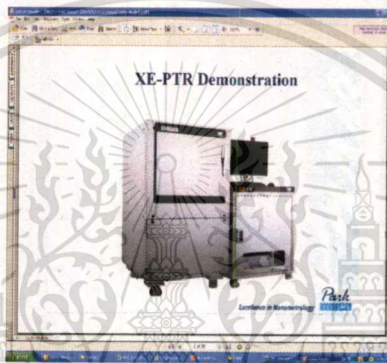
1) Figure A: Comtech machine 2460 model



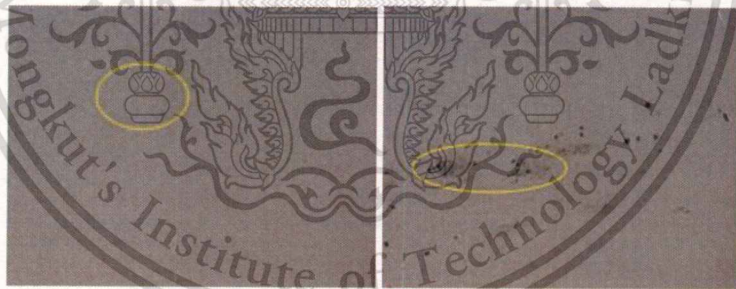
2) Figure B: Micro head Tencorr machine



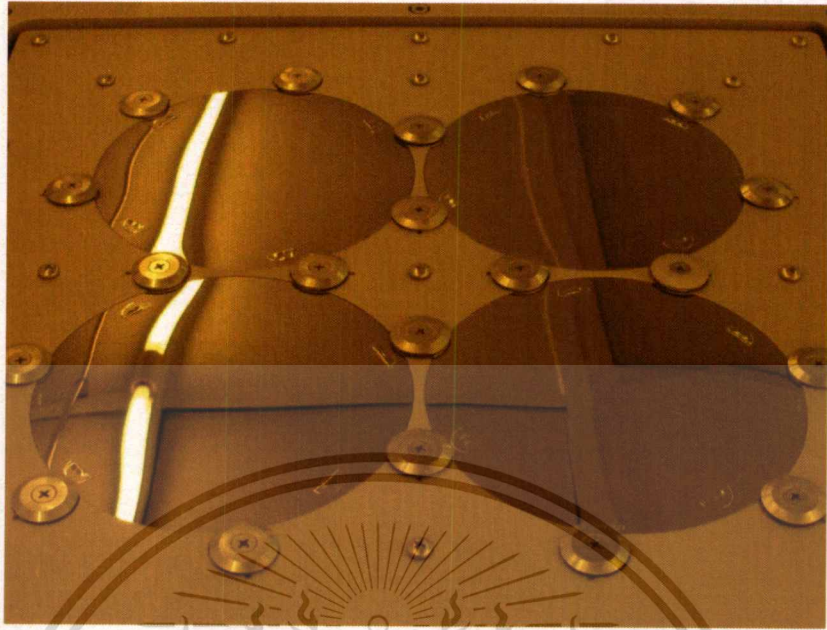
3) Figure C: SEM Model: PTM600



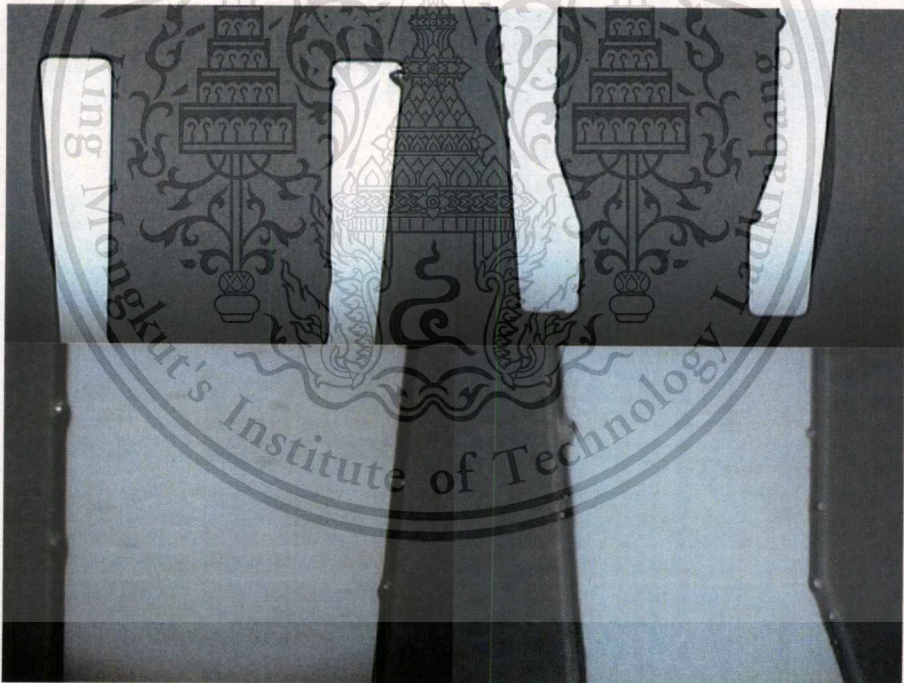
4) Figure D: AFM Model: XE-PTR



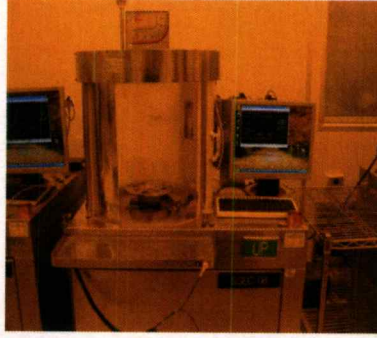
5) Figure E: Particulate contamination before – after Comtech chromium coating



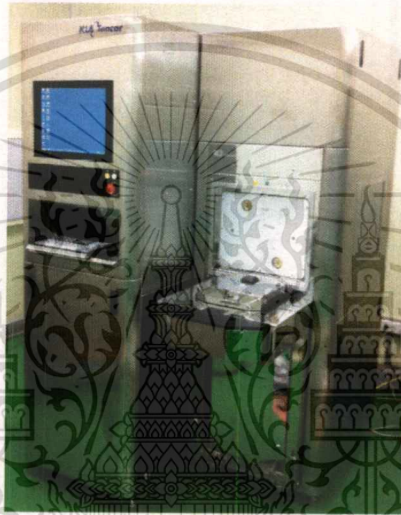
6) Figure F: Chromium wafer have deposit with chromium film



7) Figure G: Masking defect have generated from particulate contamination on chromium film then do patterning on wafer end result



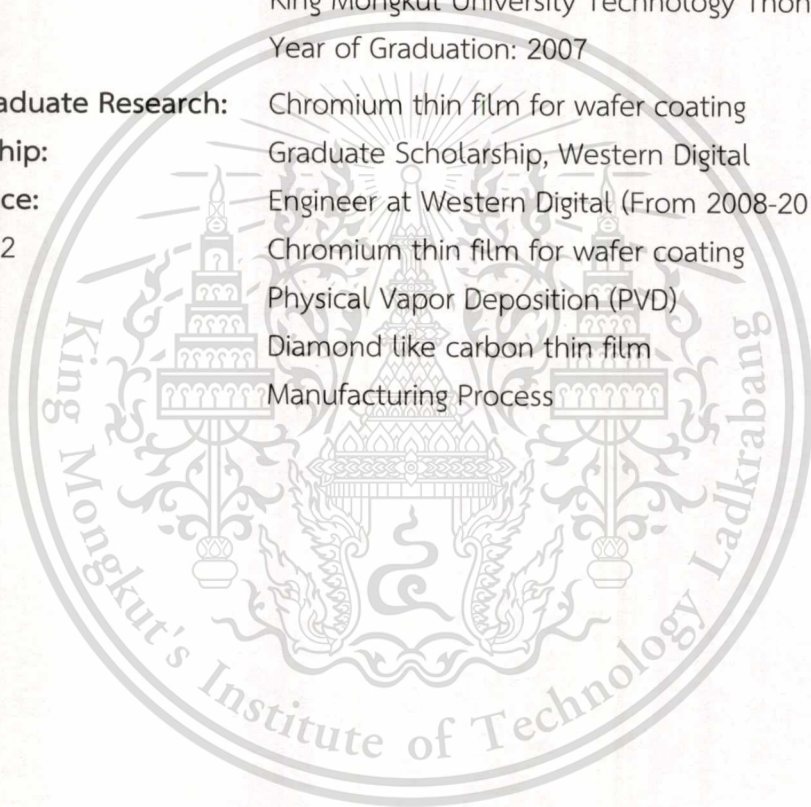
8) Figure H: Nylon brush clean wafer machine



9) Figure I: KLA particle measurement machine.

AUTHOR BIOGRAPHY

Name	Theerachai Sae-jong
Date of Birth	June 27, 1984
Address	1637 Thoerdai rd. taladploo province Thonburi district Bangkok 10600
Educational Background	2004-2008 Bachelor degree: Physics science Department of Physics Faculty of Science King Mongkut University Technology Thonburi Year of Graduation: 2007
Undergraduate Research:	Chromium thin film for wafer coating
Scholarship:	Graduate Scholarship, Western Digital
Experience:	Engineer at Western Digital (From 2008-2013)
2008-2012	Chromium thin film for wafer coating
2009	Physical Vapor Deposition (PVD)
2008	Diamond like carbon thin film
2008	Manufacturing Process



KKU-IENC 2012

Certificate of Participation

This certifies that

Theerachai Sae-jong

has participated and presented the paper

“Effect of sputtering on contamination of chromium films”

which was peer reviewed at

The 4th KKU International Engineering Conference
held on May 10-12, 2012, Khon Kaen, Thailand



Assoc. Prof. Dr. Somnuk Theerakulpisut
General Chair

Dean, Faculty of Engineering,
Khon Kaen University



Effect of sputtering on contamination of chromium films in Harddisk manufacturing

Theerachai Sae-jong¹, Wisut Titiroongruang²

¹College of Data Storage innovation, King Mongkut's institute of Technology Ladkrabang Bangkok 10520, Thailand

²Faculty of Engineering, King Mongkut's Institute of Technology Ladkrabang, Bangkok 10520, Thailand
E-mail: ¹Theerachai.sae-jong@wdc.com, ²Ktwisut@kmitl.ac.th

Abstract— Particulate contamination has generated during plasma deposition caused violent problems in the fabrication of thin films product. Particles contaminate is generated in plasma deposition, especially for sputtering process. KLA machine was used to scan and measure particle size before and after coating outside sputtering chamber. FE-SEM and EDX technique were used for characterizing type of particles. The experiments can be categorized into 3 groups. First group varies processing pressure while other parameters were controlled. Second group varies substrate DC biased voltage and finally varies gap distance between substrate and target, other parameters were controlled also. This study reports on the effect of different of pressure DC bias and DC bias voltage to observe particulate contamination on the chromium film. From the experimental results, the optimum conditions for obtaining the lowest level of particulate contamination is 8 mTorr, 40 V and 1.6 inch gap distance between the substrate and the target, substrate DC bias voltage and gap distance, respectively. According to EDX results, the contamination on film surface may come from various sources, such as from target, shutter, substrate, and sputtering system component.

Keywords—RF sputtering, particulate contamination, FESEM-EDX

I. INTRODUCTION

Recently, the particle contaminate in metal film has major issued in many electronic industries, especially hard disk drive (HDD) manufacturing. The particulate contamination was studied during plasma deposition. These problems can be categorized into 2 portions. 1) Pin hole or dark spot was found on chromium surface given yield loss and scrap [1]. 2) Peel off of chromium film was found caused rework wafer with high cost. Manufacturers require more frequently maintenance the vacuum system for compensate yield lose, resulting in high cost of production. The yield losses from the particulate contamination can shift the cost of production to unsuitable [2].

Over past decade year, particle growth in sputtering plasma was studied by many researches. Discovery of particle formation and transportation in plasma deposition process and plasma etching process show both similarities and differences. Particle formation, growth and trapping in plasma deposition process are similar to plasma etching process.

Re-deposition rates on different target regions are not equal because each region has exposed to different plasma density. Particle formation produced in low plasma density region of the target. Whereas high plasma density region, the particle would be sputtered away. This mechanism may be universal to many sputtering processes [3].

II. EXPERIMENT

The Alcatel Comptech 2460 dielectric RF sputtering system was utilized for this research, as shown in Fig. 1. In parallel plate system, two electrodes, one being coupled to an RF power generator, the other being grounded, are used to create an electrical field between the electrodes. A vacuum chamber size is 30" width x 60" length x 3.5" height and fabricated from non-magnetic type 304 stainless steel. Inside the vacuum chamber is a shutter assembly consisting of an aluminum flat plate which can be positioned between a target holder and a substrate holder during pre-sputtering and pre-clean processing

The target and substrates were loaded face up onto a square 17" x 17" nickel plated oxygen-free high thermal conductivity (OFHC) copper substrate holder. The substrates held in place by retaining stainless steel 304 screw and alumina (Al₂O₃) button. The substrate loading capacity is 4 wafers for a cycle. The substrate holder was placing 0.6" above the target. The target was made of Chromium purity 99.95% with a dimension of 17" x 17". Aluminium titanium carbide (AlTiC) round wafer 6" diameter and 1.2 millimeters thick was used as the substrate.

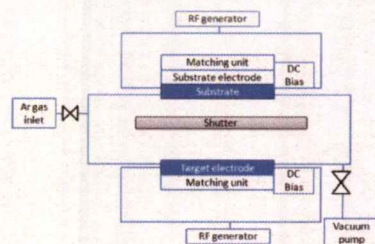


Fig.1 Schematic of Alcatel Comptech 2460 RF sputtering

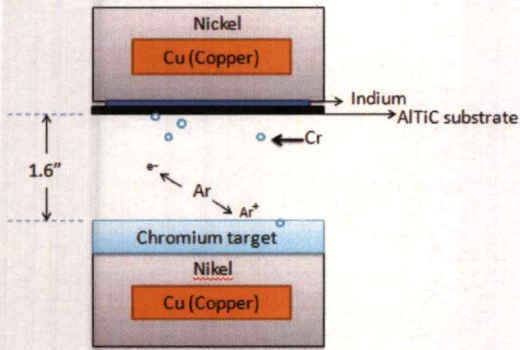


Fig.2. Schematic of target and substrate electrode.

Substrate surface was prepared by isopropyl alcohol immersion for 20 min and then cleaned by brushing deionization water spin rinse dry, followed by moisture released in vacuum pumping more than 7×10^{-2} Torr total 5 minutes, respectively. Measurement of particle contamination on the substrate surface before coating was also required.

The KLA machine used to scan and measure particle size after coating. The KLA scanning particle was done outside sputtering chamber. A light source is laser with 633 nm wavelength. Laser spot size is approximately 5 μm . The substrates were put on permaluk state and held in place by vacuum system. State was set to rotate 3200 rpm during scanning. Because of rotating 3200 rpm, dust or particles outside chamber that may fall on the film surface after finishing coating are negligible since they will be blow away during scanning. The size of particulate contamination less than 3 μm is negligible because, the minimum particle size that KLA can detect is equal or larger than 3 μm .

To identify the source of contamination, the particulate contamination on the Chromium film surface was characterized by FE-SEM with EDX mode. The Alcatel Comptech 2460 dielectric RF sputtering has not real time thickness measurement system because there is no ellipsometry inside the chamber. Then all recipe were set sputtering time at 15 min. The sputtering conditions were varied only interested parameter but fix other parameters. The experiment was divided into 3 groups. Group 1 varied processing pressure while other parameters were controlled. Group 2 varied substrate DC bias voltage and group 3 varied gap distances between target and the substrate, other parameters were controlled also.

The substrates coated with Chromium films were randomly selected to characterize and identify the contamination source. The particulate contaminations observed by KLA, cannot be observed by eyes view. Therefore, all of them were investigated through light power microscopy with magnification 50X and characterized by FE-SEM & EDX.

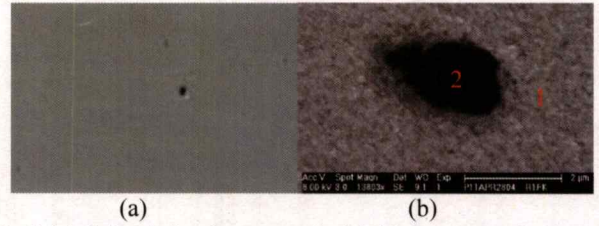


Fig 3 (a) Point defect is captured with high power microscopy and (b) SEM image show hole inside Cr film with approximately 56 μm diameter The EDX detail at point 1 show composition of Cr, but at point 2 show composition of Cu substrate.

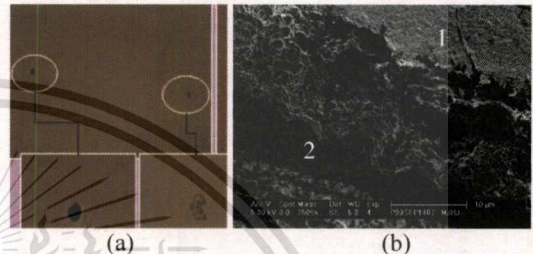


Fig 4 (a) Dark spot contamination is taken under high power microscopy. (b) SEM image show approximately 10 μm length. The EDX detail at point 1 show a composition of Cr film. But at point 2 show Cr and C. Dark spot contamination may generate from chamber material or human who load/unload substrate to sputtering machine. Film deposition on the walls of the plasma chamber can flake due to thermal expansion mismatch, film stress, or from poor adhesion of the film to the wall.[4]

III. RESULT/DISCUSSION

The particulate contamination was observed by KLA particle scanning and measurement.

Processing pressure varying 8 20 and 30 mTorr respectively was investigated. It found that the lowest level of contamination can be obtained at 8 mTorr. It shows contrast result with theory as we known that operating under low pressure as possible provides the most pure condition. This phenomenon is due to the particulate contaminations observed on film surface.

For substrate biased voltage, varying from 40 to 120 with increment of 40 volt was investigated. The results reveal the particle minimum at 40V. The distance between Substrate and target distance is various 1inch 1.3 inch and 1.6 inch with RF power 1.5 kW. Particulate contaminations especially decrease at 1.6 inch when compared with 1 inch and 1.3 inch . Low substrate DC bias voltage make electric charge particle have low kinetic energy then the possibility of particle falling into or onto film surface is also lower than high DC bias voltage.

An ionization of Ar does direct change with RF power on target. The lowest RF power show small quantity of an ionization of Ar. The system runs with low energy, the possibility of particle moving to film surface is also lower.

The substrate positions in a sputtering chamber were also investigated. The Alcatel Comptech 2460 dielectric RF sputtering system was designed to load 4 substrates per run. It

was also designed Ar gas inlet near the substrate position 1. Vacuum pump system link to the sputtering chamber at the position between substrate position 3 and 4, as shown in Fig. 5. Moreover, the contaminations before coating were not overlooking. Since substrates have cleaned before coating till reach acceptable level of contamination. The particulate contamination after coating observed from the KLA machine was expected to generate from sputtering environment. The correlation of contamination before and after coating was considered.

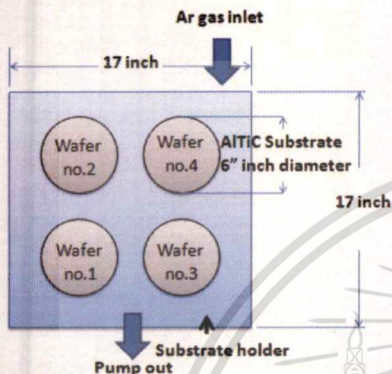
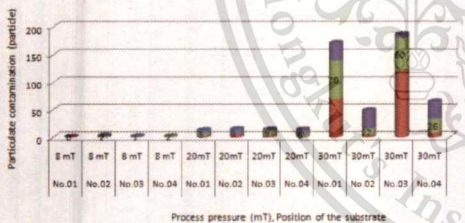


Fig. 5 Substrate position in sputtering chamber.

The experimental results as revealed in Fig. 6, the particle fall minimum on the film surface with 8 mTorr. Particulate contamination was increased at 20 mTorr 30mTorr respectively.

The relation between pressure and particulate contamination on the chromium film



(Fig. 6 a)

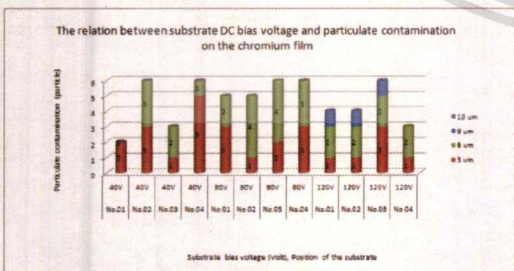


(Fig.6 b)

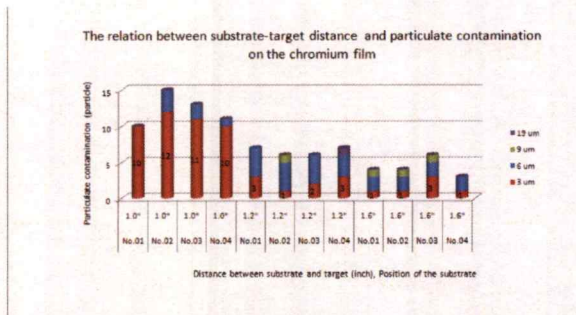


(Fig.6 c)

Fig.6. Particulate contamination before and after coating at different substrate position, (6 a: group1 varied process pressure, 6 b: group 2 varied substrate DC bias voltage, 6 c: group 3 varied gap distance between target and the substrate.)

IV. CONCLUSION

Previously, we have known that sputtering plasma can be generating particle. In this study, various sputtering conditions were considered as the effect on particulate contamination in chromium metal film. KLA scanning and measurement machine is used for quantify particle. From the result, the lowest level of particulate contamination of each parameter is 8mT, 1.6 inch gap distance between the Substrate and chromium target respectively. This experiment should have further study for finding the optimum condition by setting design of experiment (DOE) since this research consider each parameter at a time. Particulate contaminations are generated from several sources such as target material, sputtering system component and loading substrate procedure. Further study is recommended to quantify major source of particulate contamination.

ACKNOWLEDGMENT

This work was funded by DSTAR, KMITL and also supported by Western Digital (WD).

REFERENCES

- [1] W. J. Bertram "VLSI Technology" (ed. S. M. Sze), McGraw-Hill. pp. 600-605 (1983).
- [2] J. F. O'Hanlon and H. Parks. J. Vac. Sci. Technol. A. 10. 1863 (1992).
- [3] G. S. Seiwyn "particle contamination formation and detection in magnetron sputtering processed", International thin film conference
- [4] G. S. Seiwyn, "Particles and Gases and Liquids 3: Detection. Characterization and Control", (ed. K. L. LMittal), Plenum Press, pp 213-222 (19931, and references therein.